Journal of Medicinal Chemistry

Article

Selective mode of action of guanidine containing non peptides at human neuropeptide FF receptors

Findeisen Maria, Würker Cäcilia, Daniel Rathmann, Meier René, Jens Meiler, Roger Olsson, and Annette G. Beck-Sickinger

J. Med. Chem., **Just Accepted Manuscript** • DOI: 10.1021/jm300535s • Publication Date (Web): 18 Jun 2012

Selective mode of action of guanidine-containing non-peptides at human NPFF receptors

Maria Findeisen[†,⊥], *Cäcilia Würker*[†,⊥], *Daniel Rathmann*[†], *René Meier*[†], *Jens Meiler*[‡], *Roger Olsson*[§] *and Annette G. Beck-Sickinger**[†]

† Institute of Biochemistry, Faculty of Biosciences, Pharmacy and Psychology, Leipzig University, Brüderstrasse 34, D-04103 Leipzig, Germany

‡ Vanderbilt University, Center for Structural Biology, 5144B Biosci/MRBIII, 465 21st Avenue South, Nashville, TN 37232-8725, USA

§ ACADIA Pharmaceuticals Inc., 3911 Sorrento Valley Boulevard, San Diego, California 92121, and Medicinal Chemistry, Faculty of Science, University of Gothenburg, PO Box 460, SE-405 30 Gothenburg, Sweden

Author Contributions.

⊥ These authors contributed equally to this work, joint first authors.

RECEIVED DATE

ABBREVIATIONS USED. ACN, acetonitrile; CHO cells, Chinese hamster ovary cells; COS-7 cells, African green monkey kidney fibroblast cells; DMEM, Dulbecco`s modified Eagle medium; ECL, extracellular loop; E_{max}, maximum efficacy; EtOH, ethanole; FCS, fetal calf serum; HEK-293T cells, human embryonic kidney 293T cells; ICL, intracellular loop; IP, inositol phosphate; NPAF, neuropeptide AF; NPFF, neuropeptide FF; $NPFF_1R$, neuropeptide receptor subtype 1; $NPFF_2R$, neuropeptide receptor subtype 2; NPSF, neuropeptide SF; NPVF, neuropeptide VF; REU,

Rosetta Energy Units; RP-HPLC, reversed phase high performance liquid chromatography; R-SAT, receptor selection and amplification technology; SEM, standard error of the mean; SPPS, solid-phase peptide synthesis; TM, transmembrane; wt, wildtype

AUTHOR INFORMATION.

To whom correspondence should be addressed. Annette G. Beck-Sickinger, Universität Leipzig, Faculty of Biosciences, Pharmacy and Psychology, Institute of Biochemistry, Brüderstraße 34, 04103 Leipzig, Germany. Phone: 0049-341-9736900. Fax: 0049-341-9736909. E-mail: beck-sickinger@uni-leipzig.de.

ABSTRACT

The binding pocket of both NPFF receptors was investigated, focusing on subtype-selective behavior. By using four non-peptidic compounds and the peptide mimetics RF9 and BIBP3226 agonistic and antagonistic properties were characterized. A set of Ala receptor mutants was generated, the binding pocket was narrowed down to the upper part of transmembrane helices V, VI, VII, and the extracellular loop 2. Positions 5.27 and 6.59 have been shown to have a strong impact on receptor activation and were suggested to form an acidic, negatively charged binding pocket in both NPFF receptor subtypes. Additionally, position 7.35 was identified to play an important role in functional selectivity. According to docking experiments, the aryl group of AC-216 interacts with position 7.35 in the $NPFF_1$ but not in the $NPFF_2$ receptor. These results provide distinct insights into the receptor specific binding pockets, which is necessary for the development of drugs to address the NPFF system.

INTRODUCTION

RFamide peptides are biologically active peptides that share a common carboxy-terminal Arg-Phe-amide motif and vary in their N-terminal length. The mammalian octapeptide neuropeptide FF (NPFF; FLFQPQRF-NH_2) belongs to the RFamide family and was first characterized and isolated in 1985 from bovine brain by immunoreactivity using anti-FMRFamide-antisera.[1] The NPFF receptor system is involved in numerous physiological functions such as cardiovascular actions,[2,3] regulation of body temperature[4,5] and water balance.[6,7] As NPFF plays an important role in the modulation of pain and the regulation of the opioid system, it represents a peptide with strong therapeutic potential (for review see Findeisen *et al*, 2011[8]). Despite these findings, there is no significant affinity of NPFF for any of the opiate receptor subtypes.[9,10] Instead, NPFF interacts with two subtypes of $G_{i/o}$-protein coupled receptors, $NPFF_1R$ and $NPFF_2R$, which share approximately 50% sequence identity.[11] Further sequence homology of the NPFF receptor system was found among the closely related receptors of the neuropeptide Y, orexin and cholecystokinin families (31 – 37% similarities).[11] Up to now, two precursors (pro-$NPFF_A$ and pro-$NPFF_B$) have been cloned, which generate different RFamide peptides such as NPAF (AGEGLNSQFWSLAAPQRF-NH_2), NPSF (MPHSFANLPLRF-NH_2) and NPVF (VPNLPQRF-NH_2).[12,13,14,15] Although NPFF and NPVF exhibit high binding affinities for both NPFF receptor subtypes, it has been shown that peptides derived from pro-$NPFF_B$ (NPVF, NPSF) were found to slightly prefer binding to the $NPFF_1R$, whereas $NPFF_2R$ favors peptides generated from pro-$NPFF_A$ (NPFF, NPAF).[11,13] In a quantitative autoradiographic study using [^{125}I]YVPNLPQRF-NH_2 and [^{125}I]EYFSLAAPQRF-NH_2 as selective radioligands, NPFF receptors were shown to be widely expressed in the central nervous system but only the $NPFF_2R$ has been detected spinally.[16] Accordingly, it is presumed that the activation of $NPFF_2R$ results in an antinociceptive phenotype, whereas the pronociceptive actions of NPFF are driven by the activation of $NPFF_1R$.[13,17]

Recently, several small non-peptidic compounds with varying selectivity for $NPFF_1R$ and $NPFF_2R$ have been described.[17,18] Systemic administration of the selective $NPFF_2R$ agonists AC-093 and AC-099 increased hypersensitivity in neuropathic and inflammatory pain models in rats.[17,18] Likewise, the

selective $NPFF_1R$ antagonist AC-970 was demonstrated to mediate antinociceptive effects such as reversing established mechanical allodynia by attenuating spinal nerve ligation induced mechanical hypersensitivity in rats.[17] Contrarily, systematic administration of an unselective NPFF receptor subtype agonist (close analog of AC-216) increases sensitivity to noxious thermal and non-noxious mechanical stimuli and was shown to potentiate allodynia in neuropathic rats.[17,18] Therefore, selective $NPFF_1R$ antagonists and/or $NPFF_2R$ agonists might be promising for the treatment of chronic pain.[17] The most frequently investigated ligands however, are BIBP3226[19,20] and RF9,[21] as they were found to display high affinities for the NPFF receptors. As the structures of RF9 and BIBP3226 resemble the C-terminal RFamide motif, they can be also used as a tool for the investigation of crucial residues within the receptor binding site.[22]

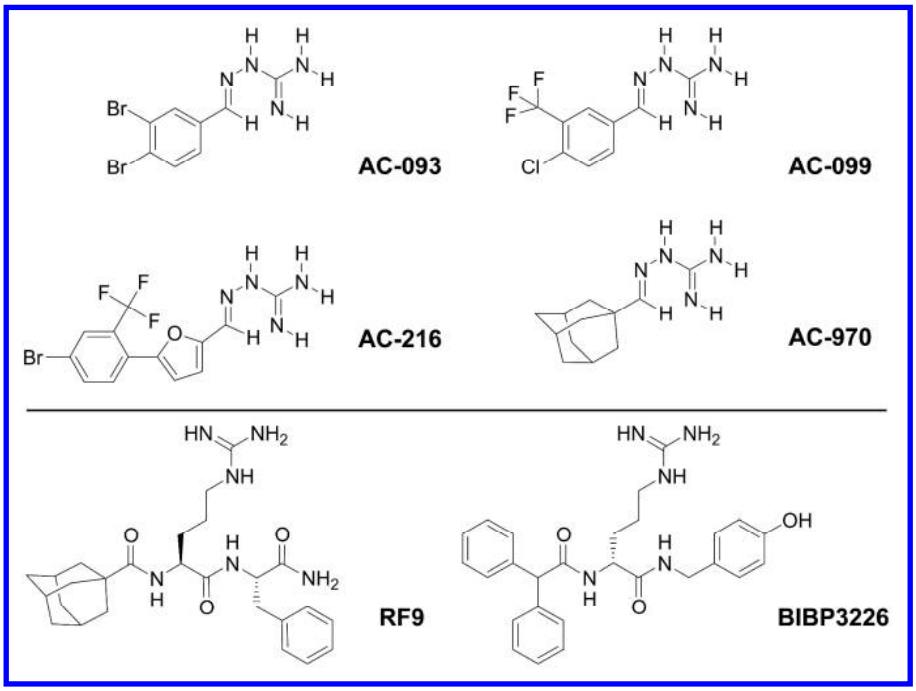

Figure 1. Structures of AC-093, AC-099, AC-216, AC-970, RF9 and BIBP3226.

The aim of the current study was the identification of the binding mode at $NPFF_1$ and $NPFF_2$ receptor with special focus on the differences between the receptor subtypes in order to develop more selective analogs. In addition to the most potent native ligands (NPFF, NPVF), two previously described high affinity dipeptide mimetics (RF9, BIBP3226) were used, that resemble structurally the C-terminal RFamide and are more rigid compared to the octapeptides. Furthermore, four non peptide guanidine

compounds were used, which have been reported to show distinct pharmacological profiles at both receptor subtypes.

Seven variants of both receptors with mutations in the extracellular loops 2 and 3, and the upper part of transmembrane (TM) helices V, VI or VII were generated, replacing hydrophobic or negatively charged residues by Ala. Testing of the peptides and the non-peptides led to distinct sensitivities especially at position F/Y$^{7.35}$ suggesting that this residue plays a crucial role in the receptor subtype specificity. A 3D model from available experimental GPCR structures was constructed and subsequently respective ligands were docked. Based on the models different but overlapping binding pockets for ligands in both receptors were hypothesized. Thereby these models explain the subtype selectivity of the analogs and will guide further studies to develop selective compounds.

RESULTS

Characterization of NPFF receptor ligands. The C-terminally amidated peptides NPFF and NPVF were prepared by automated solid phase peptide synthesis (SPPS) using a Rink amide resin according to the orthogonal Fmoc/*t*Bu strategy.[22] The synthesis of the small compounds has been described previously.[18] All structures of the investigated molecules are shown in Figure 1. All investigated compounds share a guanidinium group which might mimic the C-terminal region of the RFamide motif explaining its necessity for ligand binding. The substituted phenyliminoguanidines AC-093 and AC-099 carry electron withdrawing substituents in position 3 and 4 such as bromo, chloro or trifluoromethyl groups.[18] The aryliminoguanidine AC-216 belongs to the subclass of 5-aryl substituted-five-membered heteroaromatic iminoguanidines and is a close analog of the recently described compound 9,[18] carrying an additional bromine substituent. Furthermore, a lipophilic adamantane structure is present in AC-970. Likewise, RF9 carries an adamantanecarbonyl moiety and moreover resembles the characteristic C-terminal RF-amide dipeptide motif. The structurally related BIBP3226 carries a diphenylacetyl group and a hydroxybenzyl moiety at its argininamide backbone.

***In vitro* characterization confirms subtype-dependent activity of compounds AC-093, AC-099 and AC-970 in the NPFF receptor system, whereas AC-216 acts in a nonselective manner.** Concentration-response curves of IP accumulation assays were performed up to 31.6 μM for compounds AC-970 and AC-216, whereas AC-093 and AC-099 were tested up to concentrations of only 10 μM, owing to the cytotoxic effects of these compounds in a resazurin-based cell viability assay at higher concentration (Table S1, Figure S1). As internal reference standards NPVF at $NPFF_1R$ and NPFF at $NPFF_2R$ were used. Investigating the subtype-selective behavior of the guanidine compounds AC-970, AC-216, AC-093 and AC-099 IP accumulation assays (Figure 2) confirmed the data originally presented by using cyclic AMP inhibition assays (cAMP assays) in HEK-293T cells or receptor selection and amplification technology (R-SAT) in NIH-3T3 cells expressing $NPFF_1R$ and $NPFF_2R$, respectively.[17,18]

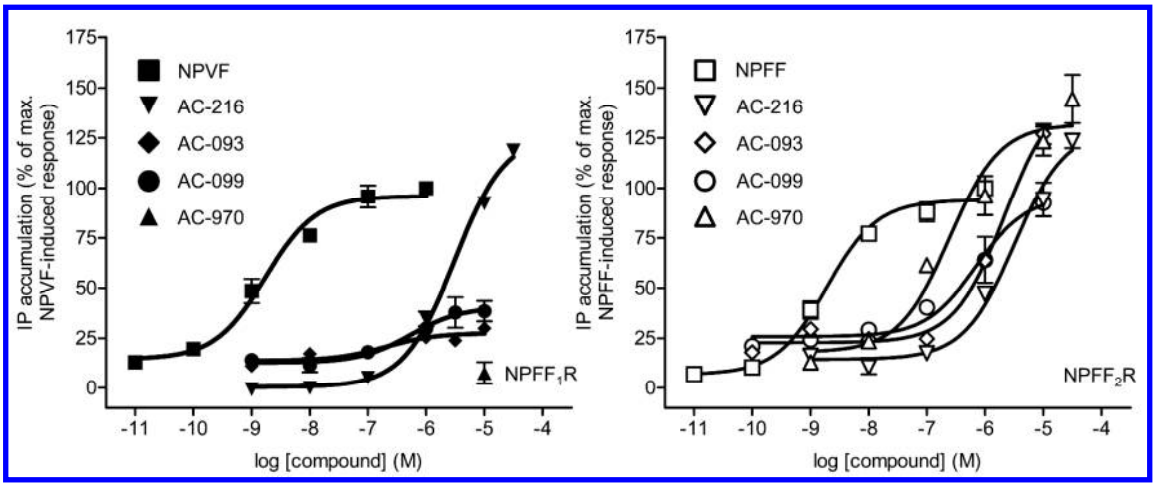

Figure 2. Representative concentration-response curves after 2 h of stimulation with small non-peptidic ligands AC-093, AC-099, AC-216 and AC-970 and endogenous ligands at human $NPFF_1R$ (left panel) and $NPFF_2R$ (right panel) in IP signal transduction assays. Results are expressed as percentage relative to maximal IP accumulation of the reference agonists and were obtained in COS-7 cells expressing NPFFR wt and chimeric G-protein as described in the Experimental Section. Concentration-response curves are obtained from data of at least two independent experiments performed in duplicates and were used to generate EC_{50} and E_{max} values, which are summarized in Table 1.

According to the results of the IP accumulation assays (Table 1), AC-970 is a full agonist at $NPFF_2R$ (EC_{50} = 298 ± 35 nM, E_{max} = 132 ± 13%) but significantly less potent at the $NPFF_1R$. For stimulation of AC-216 a full agonist behavior (E_{max}) at both NPFF receptor subtypes ($NPFF_1R$: E_{max} = 110 ± 2.9%; $NPFF_2R$: E_{max} = 118 ± 4%) was found but with significant loss of activity (EC_{50}) at $NPFF_1R$ (EC_{50} = 5624 ± 3161 nM) and at $NPFF_2R$ (EC_{50} = 1161 ± 638 nM). Compound-induced receptor response revealed a partial agonism of AC-093 (E_{max} = 22 ± 5.3%) and AC-099 (E_{max} = 40 ± 1.6%) at $NPFF_1R$, representing a 310-fold lower activity for AC-093 and 1394-fold less potency for AC-099, respectively, compared to NPVF. At $NPFF_2R$ both compounds (AC-093, AC-099) were found to fully activate the receptor but showed a significant loss of EC_{50} (1291-fold for AC-093 and 699-fold for AC-099). A 137-fold loss in receptor activity was observed for BIBP3226 at $NPFF_2R$, representing an EC_{50} value of 233 ± 3.9 nM with decreased efficacy (57 ± 7.8%) relative to NPFF-induced response at $NPFF_2R$, whereas no IP accumulation was observed at high concentrations of 10 μM at $NPFF_1R$ after stimulation with BIBP3226. RF9 showed a less distinct loss of potency of 41-fold at $NPFF_1R$ compared to a 222-fold loss of activity at $NPFF_2R$. As shown in Table 1, RF9 acts as a full agonist at $NPFF_1R$ (E_{max} = 93 ± 6.8%), whereas E_{max} values are slightly decreased for stimulation at $NPFF_2R$ (75 ± 7.5%). Due to the fact, that neither AC-970 nor BIBP3226 were able to induce receptor signaling when tested at $hNPFF_1R$, possible antagonistic properties were investigated by performing concentration-response curves of NPVF in the presence of fixed concentrations of AC-970 and BIBP3226 and found a loss of potency of 3-fold (0.1 μM), 14-fold (1 μM) and 330-fold (10 μM) for AC-970 and 12-fold (0.1 μM), 30-fold (1 μM) and 671-fold (10 μM) for BIBP3326. As efficacy was not decreased, a competitive antagonism of AC-970 and BIBP3226 at $hNPFF_1R$, respectively, was concluded. Accordingly, the Schild plot is linear with a slope close to unity for AC-970 (1.04 ± 0.19) and BIBP3226 (0.89 ± 0.05). The pA_2 value determined by nonlinear regression is 7.38 for AC-970 and 7.68 for BIBP3226, which theoretically equals the dissociation equilibrium constant.

Table 1. Comparison of potency (EC_{50}) and efficacy (E_{max}) of small guanidine compounds, BIBP3226, RF9 and endogenous ligands NPVF (VPNLPQRF-NH_2) and NPFF (FLFQPQRF-NH_2) at the human $NPFF_1$ and $NPFF_2$ receptors

Ligand	$hNPFF_1$ receptor				$hNPFF_2$ receptor		
	EC_{50} (nM)[a]	x-fold[b]	E_{max} (%)[c]	pA_2[d]	EC_{50} (nM)[a]	x-fold[b]	E_{max} (%)[c]
NPVF/NPFF	1.7 ± 0.2	**1**	100	-	1.7 ± 0.3	**1**	100
AC-093	527 ± 232	**310**	22 ± 5.3	-	2195 ± 29	**1291**	107 ± 13
AC-099	2370 ± 1291	**1394**	40 ± 1.6	-	1189 ± 343	**699**	92 ± 0.2
AC-970	ND	-	-	7.38	298 ± 35	**175**	132 ± 13
AC-216	5624 ± 3161	**3308**	110 ± 2.9	-	1661 ± 638	**977**	118 ± 4
BIBP3226	ND	-	-	7.68	233 ± 3.9	**137**	57 ± 7.8
RF9	71 ± 7.3	**41**	93 ± 6.8	-	379 ± 37	**222**	75 ± 7.5

[a]Values are the mean (± SEM) of parameters deduced by using Prism 3.0 software. ND: EC_{50} value was not determinable as no full receptor activation was observed up to concentration tested (10 μM). [b]Ratios with respect to the EC_{50} values of wt peptide: EC_{50}(compound)/EC_{50}(endogenous ligand). [c]Efficacy values are obtained at highest tested concentrations. [d]Values are obtained from Schild plots by using Schild regression. pA_2 values were determined by nonlinear regression using equation Y=X-pA_2.

Taken together, compounds AC-970, AC-216, AC-093 and AC-099 were found to behave as full agonists at $NPFF_2R$, whereas compounds AC-093 and AC-099 act as partial agonists at $NPFF_1R$. Stimulation of $NPFF_1R$ with AC-970 resulted in no IP accumulation at concentrations of 10 μM, whereas AC-216 showed full agonist receptor activation and accordingly is a nonselective agonist for $NPFF_1R$ and $NPFF_2R$. These data are in accordance with previously described results obtained with different assays.[17,18] By investigating RF9 and BIBP3226, RF9 was found to display agonistic activity at both NPFF receptor subtypes and BIBP3226 was found to behave as a partial agonist at $NPFF_2R$ and a competitive antagonist at the $NPFF_1R$ with similar properties as AC-970.

Identification of important positions of $NPFF_1R$ and $NPFF_2R$, respectively. The C-terminal RFamide of the ligands has been reported to be highly important for receptor interaction.[8] Accordingly,

interaction partners in the receptors should be aromatic or acidic residues. Owing to the knowledge from the closely related neuropeptide Y system,[23,24] either aromatic or acidic or polar residues in the extracellular loops 2 and 3, and in the upper region of the TM helices V, VI or VII were selected and individually replaced by Ala (Figure 3).

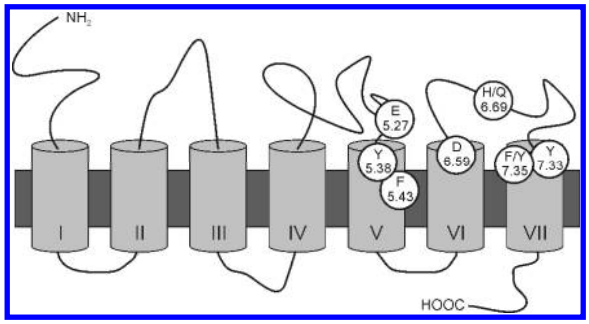

Figure 3. Schematic representation of NPFF receptor topology. Investigated positions are highlighted and numbered according to Ballesteros and Weinstein.[25]

The resulted receptor mutants were transiently expressed in COS-7 cells and functionally tested with their endogenous ligands in signal transduction assays (Table 2). The correct expression of functionally impaired receptor constructs was verified by fluorescence microscopy and confirmed to be located at the cell surface (Figure S2). Signal transduction studies of the single Ala mutants at positions $E^{5.27}$ and $D^{6.59}$ confirm the expected impact of these residues as the concentration-response curves were right-shifted compared to the wt receptors upon stimulation with NPVF and NPFF, respectively (Figure 4a). For $NPFF_1R$, mutation of Glu (EC_{50} = 7876 ± 708 nM) seems to be more dramatic than mutation of Asp (EC_{50} = 99 ± 43 nM). Furthermore, a decreased efficacy was seen relative to NPVF-induced response at $NPFF_1R$. In contrast, for $NPFF_2R$ both positions are of equal impact, resulting in an EC_{50} value of 612 ± 198 nM for $E^{5.27}$A_h$NPFF_2R$ and 341 ± 104 nM for $D^{6.59}$A_h$NPFF_2R$. Surprisingly, the $NPFF_2$ receptor mutant $D^{6.59}$A was identified to be slightly constitutively active.

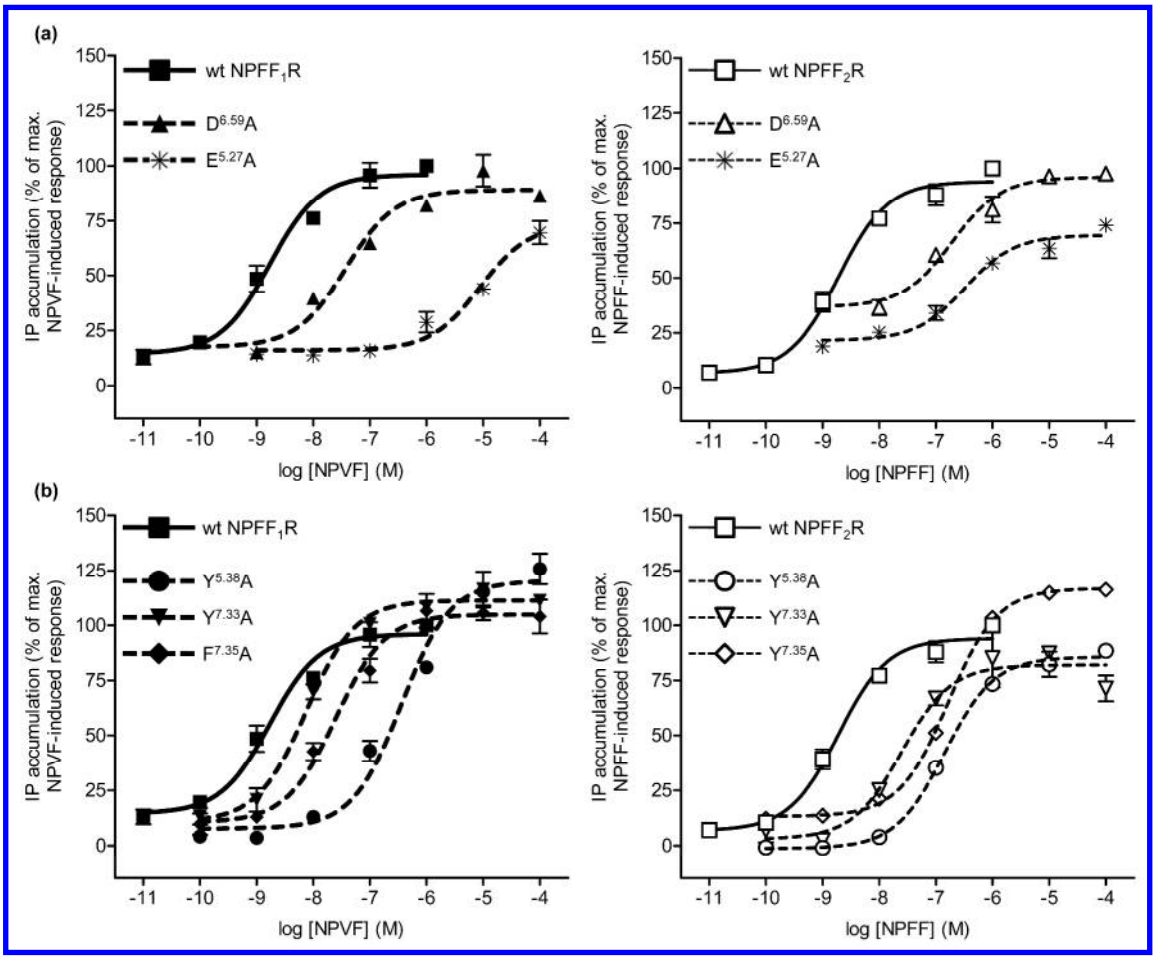

Figure 4. IP signal transduction assays were performed at wt and corresponding receptor mutants of the human $NPFF_1R$ (left panels) and $NPFF_2R$ (right panels) after stimulation with the endogenous ligands as described in the Experimental Section. Representative concentration-response curves are presented for replacement of the negatively charged residues $D^{6.59}$ and $E^{5.27}$ (panel a) as well as mutation of the aromatic amino acids $Y^{5.38}$, $Y^{7.33}$ and $F^{7.35}/Y^{7.35}$ (panel b). Results shown are expressed as percentage relative to maximal IP production of the reference agonists and were obtained in COS-7 cells expressing NPFFR wt or mutant construct and chimeric G-protein. Concentration-response curves are obtained from data of at least two independent experiments performed in duplicates and were used to generate EC_{50} and E_{max} values, which are summarized in Table 2.

Next aromatic residues were exchanged to Ala and the generated receptor mutants investigated (Figure 4b). Replacing $Y^{5.38}$ by Ala results in a significant loss in activity for $NPFF_1R$ (184-fold over wt) and $NPFF_2R$ (74-fold over wt) after stimulation with NPVF and NPFF, respectively. For $NPFF_1R$ no loss of

activity was observed at $Y^{7.33}$A_hNPFF$_1$R (EC_{50} = 4.9 ± 1.8 nM) and only a minor loss of activity at $F^{7.35}$A_hNPFF$_1$R (EC_{50} = 16 ± 6 nM). In contrast the derived NPFF$_2$R mutants were stimulated with NPFF, resulting in a loss of potency in the range of 19-fold at 7.33 (EC_{50} = 33 ± 8.5 nM) and 70-fold at 7.35 (EC_{50} = 119 ± 26 nM), suggesting a crucial role of these residues in receptor activation. Other tested mutant receptors ($F^{5.43}$A and H/$Q^{6.69}$A) showed wild type behavior at both receptor subtypes (Table 2).

Table 2. Comparison of potency (EC_{50}) and efficacy (E_{max}) of small guanidine compound AC-216, RF9 and endogenous ligands at various single point mutations of the human NPFF$_1$ and NPFF$_2$ receptors.

Construct	Ligand	hNPFF$_1$ receptor			hNPFF$_2$ receptor		
		EC_{50} (nM)[a]	x-fold[b]	E_{max} (%)[c]	EC_{50} (nM)[a]	x-fold[b]	E_{max} (%)[c]
WT	NPVF/NPFF	1.7 ± 0.2	**1**	100	1.7 ± 0.3	**1**	100
$E^{5.27}$A	NPVF/NPFF	7876 ± 708	**4632**	66 ± 2.5	612 ± 198	**360**	61 ± 9.2
$Y^{5.38}$A	NPVF/NPFF	314 ± 33	**184**	101 ± 16	126 ± 18	**74**	94 ± 7
$F^{5.43}$A	NPVF/NPFF	9.9 ± 1.4	**6**	87 ± 6.4	5.6 ± 1.3	**3**	86 ± 6
$D^{6.59}$A	NPVF/NPFF	99 ± 43	**58**	86 ± 0.3	341 ± 104	**200**	109 ± 8.2
H/$Q^{6.69}$A	NPVF/NPFF	7.7 ± 1.3	**5**	105 ± 0.6	2.7 ± 1	**2**	103 ± 1
$Y^{7.33}$A	NPVF/NPFF	4.9 ± 1.8	**2**	105 ± 7.7	33 ± 8.5	**19**	68 ± 8.2
F/$Y^{7.35}$A	NPVF/NPFF	16 ± 6	**9**	90 ± 10	119 ± 26	**70**	97 ± 6.1
WT	AC-216	5624 ± 3161	**3308**	110 ± 2.9	1661 ± 638	**977**	118 ± 4
$E^{5.27}$A	AC-216	> 10000	**-**	(21 ± 3.7)	> 10000	**-**	(24 ± 3.6)
$Y^{5.38}$A	AC-216	> 10000	**-**	(37 ± 11)	> 10000	**-**	(65 ± 11)
$D^{6.59}$A	AC-216	> 10000	**-**	(85 ± 3.7)	> 10000	**-**	(77 ± 3.9)
$Y^{7.33}$A	AC-216	4608 ± 1526	**2710**	111 ± 5.8	> 10000	**-**	(78 ± 8.7)
F/$Y^{7.35}$A	AC-216	> 10000	**-**	(88 ± 6.2)	1256 ± 40	**738**	100 ± 12
WT	RF9	71 ± 7.3	**41**	93 ± 6.8	379 ± 37	**222**	75 ± 7.5
F/$Y^{7.35}$A	RF9	462 ± 8.1	**271**	89 ± 3.8	472 ± 72	**277**	75 ± 1.2

[a]Values are the mean (± SEM) of parameters deduced by using Prism 3.0 software. WT: wildtype receptor. > 10000: EC_{50} values were not determinable as no plateau was reached up to concentrations tested. [b]Ratios with respect to the EC_{50} values of wt peptide: EC_{50}(compound)/EC_{50}(endogenous ligand). [c]Efficacy values are obtained at highest tested concentrations. E_{max} values in parentheses were estimated at 31.6 μM.

Stimulation with AC-216 and RF9 reveals subtype-selective mode of action at $F^{7.35}$A_hNPFF$_1$R and $Y^{7.35}$A_hNPFF$_2$R, respectively. As positions 5.27, 5.38, 6.59, 7.33 and 7.35 were found to be important for receptor activation to differing extents, these residues of both receptors were investigated with the unselective agonist AC-216 to gain more knowledge about functional selectivity (Table 2). Investigating $E^{5.27}$A, $Y^{5.38}$A and $D^{6.59}$A of NPFF$_1$R and NPFF$_2$R with AC-216, a further significant loss of potency for both receptor subtypes was found compared to wt receptors, respectively. Thus, $E^{5.27}$, $Y^{5.38}$ and $D^{6.59}$ are crucial residues for binding of AC-216 to both receptor subtypes, but are not relevant for subtype-selectivity. However, testing of AC-216 at $Y^{7.33}$A_hNPFF$_2$R (Figure 5a; right panel) led to a pronounced further loss of potency. Whereas, $Y^{7.33}$A_hNPFF$_1$R (Figure 5a; left panel) displayed an equipotent 2710-fold loss of potency compared to AC-216 at NPFF$_1$R, and fully activated the receptor (E_{max} = 111 ± 5.8%). A right-shifted concentration-response curve at $F^{7.35}$A_hNPFF$_1$R (Figure 5b; left panel) was observed, whereas no further decrease of potency was found at $Y^{7.35}$A_hNPFF$_2$R (EC_{50} = 1256 ± 40 nM; E_{max} = 100 ± 12%) (Figure 5b; right panel). Accordingly, AC-216 activation involves $Y^{7.33}$ and $Y/F^{7.35}$ at both receptors to a different extend.

In the studies, RF9 was found to behave as an agonist with different activities for both NPFF receptor subtypes using IP signal transduction assays. A loss of activity in the range of 271-fold for stimulation of $F^{7.35}$A_hNPFF$_1$R with RF9 (Figure 5c; left panel) was observed, displaying a further decrease in potency of RF9 at this receptor variant compared to NPFF$_1$R. Investigating the NPFF$_2$R subtype, the obtained loss of activity for stimulation of $Y^{7.35}$A_hNPFF$_2$R with RF9 (EC_{50} = 472 ± 72 nM) is in the same range as the loss of potency after stimulation of NPFF$_2$R with RF9, resulting in matching concentration-response curves (Figure 5c; right panel). As reported in Table 2, efficacy values are slightly decreased for stimulation of RF9 at $F^{7.35}$A_hNPFF$_1$R (89 ± 3.8%) and $Y^{7.35}$A_hNPFF$_2$R (75 ± 1.2%). Accordingly also for RF9 position 7.35 plays a crucial but different role at the two receptors.

Taken together, the results elucidate a nonselective mode of action of compound AC-216 at positions $E^{5.27}$, $Y^{5.38}$A and $D^{6.59}$A. Furthermore, residue 7.35 was identified to play a crucial role for binding of AC-216 and RF9 at NPFF$_1$R, whereas at the NPFF$_2$R subtype this is not the case. Thus, a

subtype-selective binding mode of AC-216 and RF9 at residue 7.35 was concluded, highlighting the importance of this position for functional selectivity.

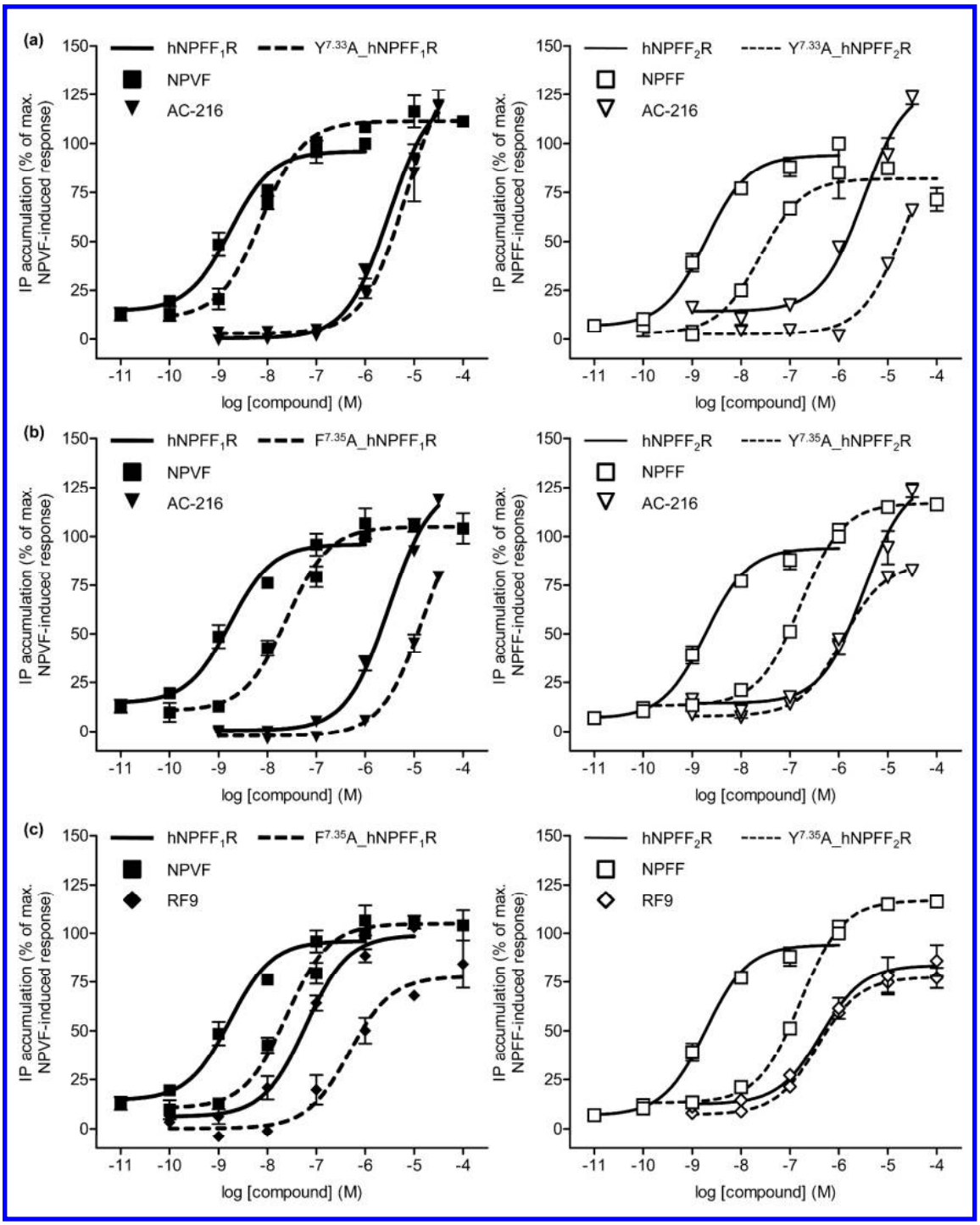

Figure 5. IP signal transduction assays were performed at wt and corresponding receptor mutants of the human $NPFF_1R$ (left panels) and $NPFF_2R$ (right panels) as described in the Experimental Section. Representative concentration-response curves are presented for stimulation of AC-216 at position $Y^{7.33}A$ (panel a) and AC-216 (panel b) and RF9 (panel c) at $F^{7.35}A\_hNPFF_1R$ and $Y^{7.35}A\_hNPFF_2R$,

respectively. Obtained data indicate a subtype-selective binding mode of AC-216 and RF9 at $F^{7.35}$A_hNPFF$_1$R and $Y^{7.35}$A_hNPFF$_2$R, respectively. Results shown are expressed as percentage relative to maximal IP production of the reference agonists and were obtained in COS-7 cells expressing NPFFR wt or mutant construct and chimeric G-protein. Concentration-response curves are obtained from data of at least two independent experiments performed in duplicates and were used to generate EC_{50} and E_{max} values, which are summarized in Table 2.

Potency is not affected by stimulation with small compound AC-970 and BIBP3226 at $Y^{7.35}$A_hNPFF$_2$R. Next, AC-970 at the NPFF$_2$R mutants was investigated to elucidate important residues of interaction (Table 3). As the replacement of $E^{5.27}$ to Ala in the NPFF$_2$R subtype resulted in a dramatic loss of activity upon stimulation with NPFF, concentration-response curves of AC-970 at this mutant were found to be right-shifted displaying an EC_{50} value > 10000 nM. Furthermore, an additional loss of potency could be observed investigating AC-970 at $Y^{5.38}$A (1440-fold over wt), $D^{6.59}$A (5211-fold over wt) and $Y^{7.33}$A of NPFF$_2$R (4901-fold over wt) in comparison to AC-970 at NPFF$_2$R, indicating a strong importance of the investigated residues for ligand binding. In contrast, stimulation of AC-970 revealed an equipotent loss of potency at $Y^{7.35}$A_hNPFF$_2$R and NPFF$_2$R in a range of ~170 fold. Moreover, a decreased efficacy was seen for stimulation of AC-970 at $Y^{5.38}$A (69 ± 1.2%) and $Y^{7.33}$A (83 ± 1.9%) of NPFF$_2$R, whereas full receptor response was reached for $D^{6.59}$A_hNPFF$_2$R and $Y^{7.35}$A_hNPFF$_2$R.

For stimulation of BIBP3226 at $Y^{7.35}$A_hNPFF$_2$R, a 66-fold loss of activity was found, resulting in identical concentration-response curves at NPFF$_2$R and $Y^{7.35}$A_hNPFF$_2$R. Moreover, efficacy was reduced to approximately one-half that of NPFF for stimulation of BIBP3226 at $Y^{7.35}$A_hNPFF$_2$R (51 ± 5.8%), displaying a partial agonism as reported in Table 3.

Taken together, positions $E^{5.27}$, $Y^{5.38}$, $D^{6.59}$ and $Y^{7.33}$ were suggested to be of importance for receptor-interaction with AC-970, whereas residue $Y^{7.35}$ of $NPFF_2R$ might not be important. Likewise, position 7.35 was assumed to be not involved in binding of BIBP3226 at the $NPFF_2R$ subtype.

Table 3. Comparison of potency (EC_{50}) and efficacy (E_{max}) of small guanidine compound AC-970 and BIBP3226 at various single point mutations of the human $NPFF_2$ receptor.

Construct	Ligand	EC_{50} (nM)[a]	x-fold[b]	E_{max} (%)[c]
WT	AC-970	298 ± 35	**175**	132 ± 13
$E^{5.27}A$	AC-970	> 10000	**-**	(59 ± 9.5)
$Y^{5.38}A$	AC-970	2449 ± 322	**1440**	69 ± 1.2
$D^{6.59}A$	AC-970	8860 ± 1343	**5211**	140 ± 9.5
$Y^{7.33}A$	AC-970	8332 ± 2727	**4901**	83 ± 1.9
$Y^{7.35}A$	AC-970	301 ± 64	**177**	107 ± 5.8
WT	BIBP3226	233 ± 3.9	**137**	57 ± 7.8
$Y^{7.35}A$	BIBP3226	113 ± 9.3	**66**	51 ± 5.8

[a]COS-7 cells were transiently cotransfected with wt or receptor variant of $NPFF_2R$ and chimeric G protein. Values are the mean (± SEM) of parameters deduced by using Prism 3.0 software. WT: wildtype. > 10000: EC_{50} values were not determinable as no plateau was reached up to concentrations tested. [b]Ratios with respect to the EC_{50} values of wt peptide: EC_{50}(compound)/EC_{50}(NPFF). [c]Efficacy values are obtained at highest tested concentrations. E_{max} values in parentheses were estimated at 31.6 μM.

Modeling provides insight into spatial distribution of amino acids in the binding site and subtype-specific differences. Based on the known structures of eight class A GPCRs a comparative model for each of the receptor subtypes was created. The TM helices as well as extracellular loop (ECL) 1 and intracellular loop (ICL) 1 of the template structures are highly structurally conserved and the alignment to the sequences of interest shows no gaps or insertions in these regions. Furthermore, the region between $C^{5.25}$ and $P^{5.50}$ of the C-X-C chemokine receptor type 4 and the $NPFF_1R$ and $NPFF_2R$ are identical in length and the possibly structural important amino acid $P^{5.30}$ is conserved. This part forms, together with the TM helices, the binding pocket. To create the model, the primary sequence of $NPFF_1R$

and $NPFF_2R$ was threaded onto the tree-dimensional coordinates of the above mentioned regions and the remaining areas were modeled with the ROSETTA molecular modeling software using cyclic coordinate descent. Signal transduction studies identified $E^{5.27}$, $Y^{5.38}$, $D^{6.59}$, $Y^{7.33}$, and $F^{7.35}/Y^{7.35}$ to be, to a different degree, important for receptor activation. The models suggest that $E^{5.27}$, $D^{6.59}$ and $F^{7.35}/Y^{7.35}$ are directly involved in ligand binding, because they form the binding pocket. In contrast, $Y^{7.33}$ is probably not directly involved in ligand binding and faces towards TM1. $Y^{5.38}$ also forms a small portion of the binding pocket (Figure S3), but basically stabilizes the negatively charged binding pocket by interacting with Glu at 5.27 and keeping it in place. $NPFF_1R$ and $NPFF_2R$ are highly homologous receptors with only minor differences in the binding site. From the models one amino acid, namely $F^{7.35}/Y^{7.35}$, could be identified to influence substrate specificity. The consequence of this difference is that the binding pocket in $NPFF_1R$ is bigger and goes deeper into the transmembrane region compared to $NPFF_2R$ and it also shows a higher hydrophobicity as can be seen in Figure 6.

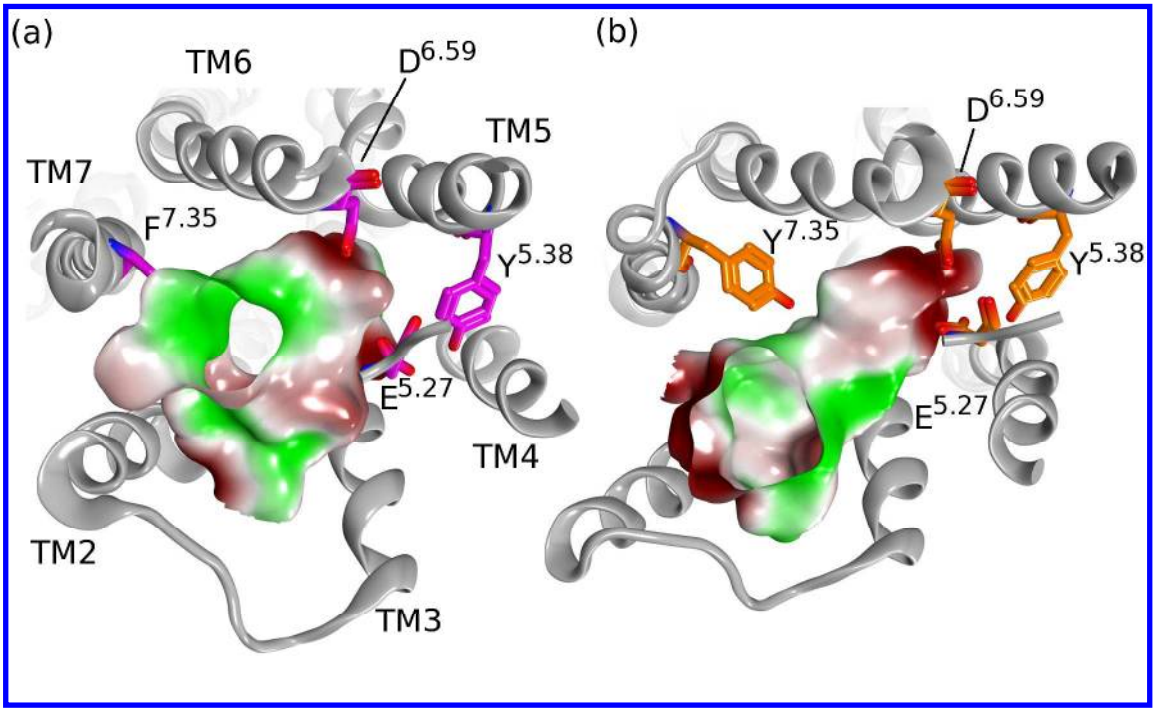

Figure 6. Shape of the binding site in the models of $NPFF_1R$ (a) and $NPFF_2R$ (b) as shown from the extracellular side. Depicted is the backbone of the receptor models in gray ribbon representation and the important amino acids which form the binding pocket in purple and orange, respectively. The solvent

accessible surface of the binding site was calculated with a 1.4 Å water probe and was colored by hydrophobicity. Hydrophobic areas are colored green and hydrophilic areas are colored red.

Docking experiments reveal different mode of binding of small guanidine compound AC-216. For each of the NPFF receptor subtypes ligand docking experiments with compound AC-216 were carried out using ROSETTA script following the ligand-docking protocol of Davis and Baker.[26] 8000 complex models were created. A statistical analysis of the interactions in the complex models showed the amino acids $E^{5.27}$, $D^{6.59}$ and $F^{7.35}$ most frequently involved in interaction in $NPFF_1R$ and the amino acids $E^{5.27}$, $D^{6.59}$ and $Y^{7.35}$ to be important for binding in $NPFF_2R$ (Figure 7). The positively charged guanidinium group of AC-216 binds to the negatively charged site between 5.27 and 6.59 via strong ionic interactions. These two important salt bridges were conserved in all low energy binding modes. In contrast, in low energy models for both $NPFF_1R$ and $NPFF_2R$ the aryl group was found in two distinct binding pockets: a pocket next to position 7.35 or in a pocket close to TM helices two and three. In conjunction with the experimental data which suggest interaction of AC-216 with $F^{7.35}$ in $NPFF_1R$, this binding mode was favored for $NPFF_1R$ while the aryl group was suggested to be in a pocket close to TM helices two and three for $NPFF_2R$. Another possible explanation is an identical binding mode of the aryl group in both receptor subtypes with a modulated binding strength at position 7.35, because the electron withdrawing effect of the hydroxyl group weakens the aromatic interaction of the aryl group with the Tyr.

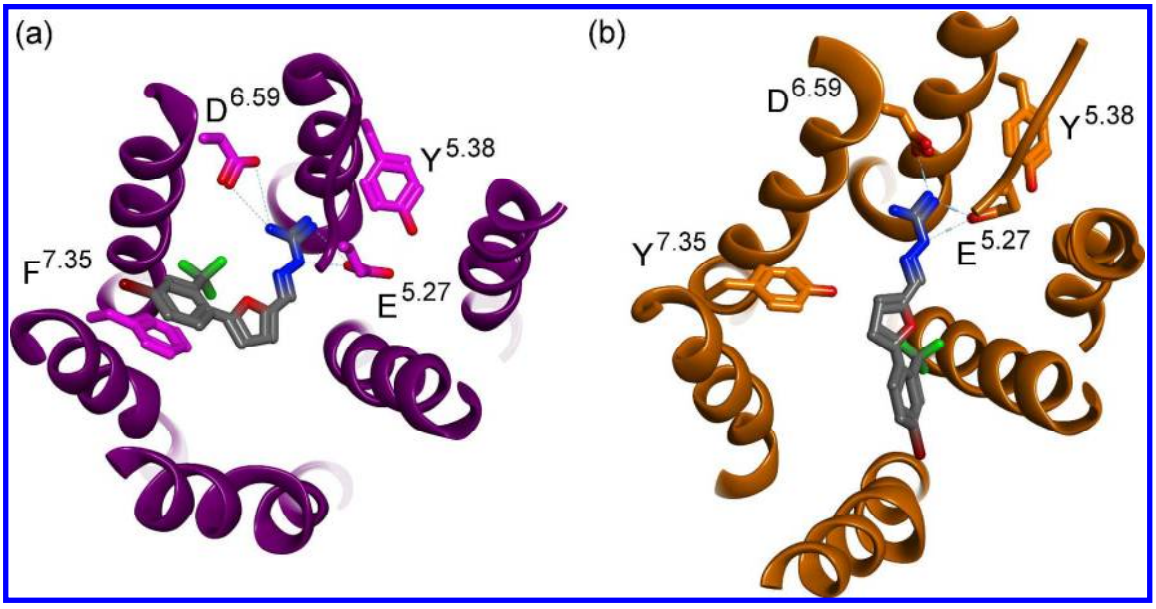

Figure 7. Model of the binding site of $NPFF_1R$ and $NPFF_2R$ in complex with AC-216. $NPFF_1R$ (a) is shown in purple and $NPFF_2R$ (b) in orange. Depicted are parts of the backbone of the seven TM helices in ribbon representation and the side chains of the amino acids forming the binding pocket in sticks. The bound ligand AC-216 as predicted from docking is shown in gray sticks.

DISCUSSION

The NPFF receptor system represents a strong therapeutic potential, as it is involved in many physiological functions. Highly selective agonists and antagonists could serve as a useful tool for the characterization of the diverse physiological roles of the NPFF receptor subtypes. The exploration of small ligands might finally enable the development of small, low molecular weight and lipophilic compounds for drug therapy. In this work, the *in vitro* activity profiles of small non-peptidic, guanidine-containing compounds were reported. Based on IP signal transduction assays and in accordance with previous work,[17,18] they could be characterized as selective $NPFF_2R$ agonists (AC-093 and AC-099), selective $NPFF_1R$ antagonist (AC-970) or unselective full agonist at both NPFF receptor subtypes (AC-216).

Data of recently disclosed R-SAT assay studies investigating selective $NPFF_2R$ agonists suggest, that 3- and 4-substituted phenyliminoguanidines, carrying electron withdrawing bromo, chloro or

trifluoromethyl groups, such as AC-093 and AC-099, show $NPFF_2R$ agonist selectivity.[17,18] These findings were confirmed by performing IP signal transduction assays. The substituted phenyliminoguanidines AC-093 and AC-099 act as full agonists at the $NPFF_2R$, while displaying only minimal activity at $NPFF_1R$ with low efficacies (Table 1). As described by Gaubert *et al*., it should be noted with caution that introducing an additional phenyl group in a phenyliminoguanidine results in an unselective behavior at both NPFF receptor subtypes.[18] These findings were confirmed as stimulation of AC-216 led to full agonistic activity at both NPFF receptor subtypes in signal transduction assays. Containing an adamantane within its structure, AC-970 was described to act as a selective $NPFF_1R$ antagonist.[18] Accordingly, AC-970 was found to behave as an antagonist at $NPFF_1R$, while exhibiting the highest $NPFF_2R$ agonistic activity of the four tested small compounds. Thus, an adamantane structure might be disadvantageous for $NPFF_1R$ induced receptor response.

In contrast, RF9, which also contains an adamantane within its structure, showed full agonist activity at $NPFF_1R$ (93 ± 6.8%) and partial agonism at $NPFF_2R$ (75 ± 7.5%) in IP accumulation assays, displaying a higher potency at $NPFF_1R$ compared to $NPFF_2R$. These findings suggest the presence of a sterically demanding substituent in addition to an adamantane structure to enhance $NPFF_1R$ activity. In contrast, it has to be considered that RF9 is reported as a potent antagonist at both NPFF receptor subtypes,[21] where RFamide derivative RF9 was inactive up to concentrations of 10 μM in cAMP accumulations assays using CHO-$hNPFF_1R$ cells and dose-dependently reversed the inhibition of forskolin-induced cAMP by NPVF.[21] Furthermore, RF9 displayed no effect on stimulation of [^{35}S]GTPγS binding to $hNPFF_2R$ membranes at concentrations up to 100 μM and a ~160-fold right-shift of concentration-effect curves was observed for NPFF in the presence of high concentrations of RF9.[21] However, in an IP accumulation assay, agonistic activity at both NPFF receptors of transiently transfected COS-7 cells after stimulation with RF9 was observed. It might be, that the differences in the functional properties in the current report compared to formerly reported studies are based on the distinct experimental systems. As mentioned above, to investigate and characterize the compounds, recombinant NPFF receptors expressed in COS-7 cells and the cotransfection of a chimeric G-protein was used to accumulate

intracellular IP. Thus, a recombinant system may be "over-expressed", leading to an agonist response, while in natural systems the receptor densities may be lower and a compound may cause no agonistic activity. Likewise, the non-peptide NPY Y_1 antagonist, BIBP3226, has been described as the first NPFF receptor antagonist based on its pharmacological properties *in vitro*. Accordingly, BIBP3226, which is structurally related to RF9 but does not contain an adamantane structure, was found to antagonize the effect of NPVF and NPFF at $NPFF_1R$ and $NPFF_2R$, respectively.[19,20] Somewhat unexpectedly, given that BIBP3226 has been proposed to be an antagonist for both NPFF receptors by its ability to reverse the inhibitory effect of NPFF on forskolin-stimulated adenylate cyclase activity in recombinant CHO cells expressing either $hNPFF_1$ or $hNPFF_2$ receptor,[20,27] it caused a concentration-dependent IP accumulation when tested in recombinant COS-7 cells expressing the $NPFF_2$ receptor (Table 1). Taken together, the antagonistic properties of BIBP3226 at $NPFF_1R$ were confirmed but a partial agonism of BIBP3226 at $NPFF_2R$ was observed. Therefore, it can be speculated that different signaling pathways of the NPFF receptors may be responsible for the distinct effects. Additionally, differences in the functionality of compounds tested at NPFF receptors were reported earlier, when the putative antagonist PFR(Tic)amide was characterized in functional assays *in vitro*.[28] The results for BIBP3226 and AC-970 observed at $NPFF_1R$ suggest both compounds to act as antagonists. Investigations with BIBP3226 showed functional antagonism for the human Y_1 receptor,[29] too. The studies reveal that BIBP3226 and AC-970 are competitive NPFF receptor antagonists that bind to the $NPFF_1R$, but do not activate the receptor.

Next, a full set of mutations has been carried out in the extracellular and transmembrane regions of the NPFF receptors. According to mutational studies at the human Y_1 receptor, BIBP3226 was suggested to interact with residue $D^{6.59}$ through its guanidinium group by mimicking the C-terminal structure of NPY.[30] Both families may have conserved an ancestral binding pocket that has evolved to the RFamide or RYamide interactions. Several mutagenesis studies performed so far suggest that the conserved $D^{6.59}$ on the top of TM helix 6 is important for receptor activation within the RFamide peptide receptor family.[8,22] In a mutational study with the prolactin releasing peptide receptor, Rathmann *et al.*

investigated the replacement of $D^{6.59}$ with Ala to result in a 22-fold loss of activity after stimulation with PrRP (unpublished data). Additionally, investigations regarding sequence conservation of the RFamide receptor family as well as the NPY receptor family revealed positions 5.27, 5.38, 7.33 and 7.35 to be interesting. Positions 5.27 and 5.38 are conserved throughout both receptor subfamilies, whereas Tyr at position 7.33 is specific for NPFF receptors. Aromaticity is often seen at position 7.35, but subtype-specific differences were found, as a Phe is present in the $NPFF_1R$ and a Tyr in the $NPFF_2R$. The models suggest receptor position 7.33 to interact with the TM helix I, thus stabilizing the functional correct conformation (Figure S3). Due to the experimental results, showing that receptor position 7.33 is important for $NPFF_2R$ activity after stimulation with NPFF, it could be proposed that this position is relevant for correct receptor conformation and the identified loss in activity seems to be the same regardless of the stimulating ligand (Figure 5a; right panel). For $NPFF_1R$ the receptor conformation is active whether Tyr or Ala is present at position 7.33, which is in good agreement to the hypothesis that this receptor position is not involved in ligand binding. According to the models, residue 5.38 does not actually bind the ligand, but is needed to activate the NPFF receptors (Table 2). Results of mutational studies for the nearby $Y^{5.39}$ in both cannabinoid receptors revealed that the aromaticity at this position is crucial.[31] The interaction of guanidinium groups with bidentate anions such as carboxylate groups can drive highly specific molecular recognition events. Positions 5.27 and 6.59 were postulated to form the negatively charged pocket, which is critical for the activation of the NPFF receptors by binding the guanidinium part of the endogenous ligands as well as of the small compounds (Figure 7). For the $NPFF_2R$ these two positions were identified to be of comparable importance (360- and 200-fold over wt). For $NPFF_1R$ mutation of Glu at 5.27 (4632- fold over wt) was found to be more sensitive to substitution than mutation of Asp at 6.59 (58-fold over wt), which is still a key residue for ligand binding. These findings are in good agreement with previous studies concerning [Xaa^7]-NPFF analogs. Those experiments have shown that substitution of Arg by Ala or Asp leads to no receptor response and minor modifications had enormous impact for both NPFFR.[22]

On the other side of the binding pocket the aromatic residue 7.35 was identified to be involved in receptor activation. Because the side chain is facing towards the binding site, it is feasible that it interacts with the bound ligand. This is proven by the loss of activity in stimulation of both Ala receptor mutants ($F^{7.35}$A_hNPFF$_1$R: 9-fold over wt; $Y^{7.35}$A_hNPFF$_2$R: 70-fold over wt) with its endogenous ligands NPVF and NPFF, respectively. As shown in Figure 5b, the concentration-response curve observed for $F^{7.35}$A_hNPFF$_1$R was right-shifted after stimulation with AC-216 compared to the wt, whereas stimulation of $Y^{7.35}$A_hNPFF$_2$R with AC-216 resulted in matching curves for wt and mutant. These findings suggest that the binding of AC-216 to $F^{7.35}$ in NPFF$_1$R is important for activation of the receptor, whereas the interaction to $Y^{7.35}$ in NPFF$_2$R is not important for binding of AC-216. This agrees well with the first experiments (Figure 2) with all compound tested at both NPFF receptors revealing that AC-093 and AC-099 are not able to induce full NPFF$_1$R response. These compounds are too small to interact with position 7.35, given that their guanidinum group binds to the negatively charged pocket between 5.27 and 6.59 (Figure 8). Nevertheless, this position is critical for activation of both receptor subtypes with their endogenous ligands, as confirmed by the loss in potency for both Ala mutants upon NPVF and NPFF stimulation, respectively.

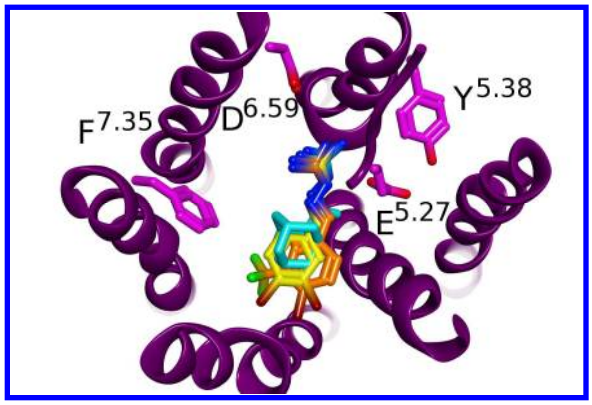

Figure 8. Model of the binding site of NPFF$_1$R in complex with AC-093, AC-099 and AC-970. NPFF$_1$R is shown in purple ribbon representation with its important amino acids highlighted as purple sticks. AC-093 is depicted in yellow sticks, AC-099 in orange sticks and AC-970 in cyan sticks.

AC-970 behaves as an antagonist as it is too short to activate the $NPFF_1R$. Given that AC-970 represents the best agonist acting at $NPFF_2R$ (Table 1), the $NPFF_2R$ mutants were investigated with the compound and the same behavior as for AC-216 tested at $NPFF_2R$ mutants was obtained. Binding of AC-970 and AC-216 do not participate at position $Y^{7.35}$ as matching concentration-response curves were observed compared to stimulation of wt $NPFF_2R$. As the structures of RF9 and BIBP3226 resemble the C-terminally characteristic RFamide motif, they can be used as a tool for the investigation of crucial residues within the receptor binding site.[22] BIBP3226 was found to act as an antagonist at $NPFF_1R$ and as a partial agonist at $NPFF_2R$. Accordingly, $Y^{7.35}$A_h$NPFF_2R$ was investigated with BIBP3226 and again no additional right-shift was observed compared to wt stimulation. With respect to the experimental data (Figure 5c) the same mode of action for RF9 could be proposed, because non-matching curves for $F^{7.35}$A_h$NPFF_1R$ after stimulation with RF9 were seen compared to the wt and matching concentration-response curves at $Y^{7.35}$A_h$NPFF_2R$. Taken together, the results suggest that binding of AC-216 and RF9 to $F^{7.35}$ in $NPFF_1R$ is important for receptor activation, whereas neither AC-216, AC-970, BIBP3226 nor RF9 are involved in binding to $Y^{7.35}$ in $NPFF_2R$.

Traditional receptor theory characterizes ligands regarding to their functional effects as full, partial, inverse agonists or antagonists and posits a model in which a certain receptor subtype is consistently associated with a single functional response. More recent data indicate that different ligands may have the capacity to invoke diverse signaling responses by selectively activating multiple effector pathways coupled to a single receptor subtype.[32,33,34] This phenomenon, also referred to as functional selectivity or agonist trafficking, has become an important tool for the characterization of receptor function and a fundamental assumption for drug development. There is a large number of receptor systems which have been observed to differently activate associated signal transduction pathways such as opioid,[35] octopamine,[36] vasopressin,[37] dopamine,[38,39] β_2-adrenergic[40] and serotonin[32,41,42] receptor families. The NPFF receptor system represents another subset of GPCRs in which functional selectivity has been observed.[43]

CONCLUSIONS

As the ability to undergo crosstalk is high within the family of RFamide peptides, the investigation of selective agonists and antagonists is necessary to elucidate distinct interactions and clarify diverse pharmacological effects. Thus, small non-peptidic compounds are suitable tools for exploring functional selectivity and defining the biological roles of NPFF receptors, as they are not subject to peptidolytic degradation and therefore metabolically stable. In this study, the subtype-selective properties of the small compounds AC-093, AC-099 and AC-970 as well as the nonselective behavior of AC-216 in the NPFF receptor system were confirmed. Moreover, a competitive antagonism of AC-970 and BIBP3226 at $NPFF_1R$ was disclosed. Surprisingly, a partial agonism of BIBP3226 at $NPFF_2R$ was observed and agonistic properties of RF9 at both NPFF receptor subtypes were found contrary to expectations from literature. Furthermore, important residues involved in ligand recognition and receptor activation were identified. Among these residues, positions 5.27 and 6.59, forming an acidic, negatively charged binding pocket, have a strong impact on receptor activation in both NPFF receptor subtypes to differing extents. Moreover, position 7.35 was identified to play an important role in functional selectivity within the NPFF receptor system by revealing a subtype-selective binding mode of RF9 and small compound AC-216. According to docking experiments, the aryl group of AC-216 interacts with position 7.35 in the NPFF receptor subtype 1 but not in the $NPFF_2R$ and therefore the presence of an aromatic residue was presumed to be responsible for substrate-specifity. In conclusion, the data provide further insight into functional selectivity in the NPFF receptor system, which is necessary for the development of selective $NPFF_1R$ antagonists and $NPFF_2R$ agonists as potential drugs for the treatment of chronic pain.

EXPERIMENTAL SECTION

Peptide Synthesis. NPFF (FLFQPQRF-NH_2) and NPVF (VPNLPQRF-NH_2) were prepared by automated multiple solid-phase peptide synthesis (SPPS) on a Syro II peptide syntheziser (MultiSynTech, Bochum, Germany) according to the 9-fluorenylmethoxycarbonyl-tert-butyl (Fmoc/tBu) strategy using a Rink amide resin (15 μmol scale) as previously described.[22] Purification of

the peptides was performed by preparative RP-HPLC (Vydac RP18-column, 22 × 250 mm, 10 µm/ 300 Å, Grace, Deerfield, IL, USA or Phenomenex Jupiter 10 U Proteo column, 250 × 21.20 mm, 90 Å, Aschaffenburg, Germany) using 0.1% (v/v) TFA in H_2O (eluant A) and 0.08% (v/v) TFA in ACN (eluant B). Both peptides were obtained with purities ≥ 95% and identified by MALDI-ToF mass spectrometry (Ultraflex III MALDI-TOF/TOF, Bruker Daltonics, Billeria, MA, USA).

Compounds. (R)-N(2)-(diphenylacetyl)-N-[(4-hydroxyphenyl)-methyl]-argininamide (BIBP3226) was purchased from Tocris (Ellisville, MO). 1-Adamantanecarbonyl-RF-NH_2 (RF9) was synthesized as described. The compounds AC-970, AC-216, AC-093 and AC-099 were kindly provided by Prof. R. Olsson (Department of Medicinal Chemistry/ University of Gothenburg/ Sweden) and synthesized by ACADIA Pharmaceuticals AB. (Malmö, Sweden).[17,18]

Resazurin-based cell viability assay. The cytotoxicity profiles of the small non-peptidic compounds were obtained by using a resazurin-based *in vitro* toxicology assay kit (Sigma-Aldrich, Taufkirchen, Germany). Therefore, COS-7 cells were seeded into 96-well plates (30,000 cells/well), grown to subconfluency under standard growth conditions and then incubated for 2 h with varying concentrations of compound solutions in DMEM containing 4.5 g/L glucose and L-glutamine supplemented with 10% (v/v) heat inactivated FCS. As positive and negative controls the cells were treated with 70% EtOH for 10 minutes or medium containing FCS. After incubation the cells were washed twice with medium without FCS and incubated for 2 h at 37°C with a 10% solution of resazurin in medium without FCS. For determination of cell viability the conversion of the nonfluorescent redox dye resazurin by metabolically active cells to reduced and highly fluorescent resorufin was measured fluorometrically at 595 nm emission wavelenghts with 550 nm excitation wavelenghts using a Spectraflour plus multiwell reader (Tecan, Crailsheim, Germany).

Cloning of expression vectors and generation of NPFFR variants. Generation of the eukaryotic expression vectors $hNPFF_1R$_EYFP_pVitro2 and $hNPFF_2R$_EYFP_pVitro2 was performed as recently described.[22] Point mutations were introduced into the $NPFF_1R$ and $NPFF_2R$ sequence by replacement of $E^{5.27}$, $Y^{5.38}$, $D^{6.59}$ and $Y^{7.33}$ to Ala using the QuickChange™ site-directed mutagenesis (Stratagene, La

Jolla, CA). For position 7.35 Phe in the $NPFF_1R$ sequence and Tyr in the $NPFF_2R$ sequence are present, which were exchanged to Ala alike. Residues were numbered according to the system of Ballesteros and Weinstein.[25] In the Ballesteros-Weinstein nomenclature the most conserved residue in each helix had been given the number 50. Correctness of all constructs was confirmed by sequencing the entire coding sequence using an ABI 310 automated sequencer.

Cell Culture. COS-7 cells (African Green Monkey Kidney Fibroblast Cells) were grown in monolayers in 75cm² culture flasks at standard growth conditions (37°C in a humidified atmosphere of 5% CO_2) and split when confluent. For dissociation and detachment of confluent cells Trypsin/EDTA (0.05%/0.02% in Phosphate-buffered saline) was used. COS-7 cells were cultured in DMEM containing 4.5 g/L glucose and L-glutamine supplemented with 10% (v/v) heat inactivated Fetal Calf Serum (FCS), 100 U/mL penicillin and 100 µg/mL streptomycin. Cell media and supplements were purchased as follows: Dulbecco`s modified eagle medium (DMEM), Dulbecco`s phosphate buffered saline (PBS), Fetal Calf Serum (FCS) and Trypsin/EDTA (0.05%/0.02% in PBS) were ordered from PAA Laboratories GmbH (Pasching, Austria). 48-well plates, 96-well plates and cell culture flasks ($75cm^2$) were supplied from TPP (Trasadingen, Switzerland).

Inositol phosphate accumulation assays. For signal transduction studies, COS-7 cells were seeded into 48-well plates (60,000 cells/well) and grown to subconfluency under standard growth conditions. The assay was performed as previosly described.[22] The compounds were initially dissolved in dimethyl sulfoxide (DMSO) and finally diluted in DMEM (10 mM LiCl) to result in 1% (v/v) DMSO. Data were analyzed using GraphPad Prism 3.0 (GraphPad Software, San Diego, CA). Concentration-response curves were fitted to a nonlinear regression model resulting in the obtained EC_{50} and E_{max} values reported. Signal transduction assays were repeated at least twice independently and performed in duplicates.

Fluorescence microscopy. HEK293 cells (120,000 cells/well) were seeded into 8-well chamber slides (ibidi, Munich, Germany) and were transiently transfected with 1 µg plasmid DNA and 1 µL Lipofectamin™ 2000 transfection reagent (Invitrogen, Karlsruhe, Germany). Fluorescence images were

obtained using an ApoTome Imaging System with an Axio Observer microscope (Zeiss, Jena, Germany). All investigated receptor constructs were correctly integrated in the cell membrane as confirmed by live-cell imaging.

Comparative modeling and docking. Comparative models were constructed for both receptor subtypes by threading the sequences through the three-dimensional coordinates of eight known GPCR structures. The following PDB IDs were selected: 2YDV,[44] 3ODU,[45] 2RH1,[46] 1U19,[47] 2Y00,[48] 3RZE,[49] 2Z73,[50] and 3PBL.[51] The alignment of target and template sequences was constrained by the highly conserved residues used in the nomenclature of Ballesteros and Weinstein[25] and the cysteins in ECL2 and TM3 forming the highly conserved disulfide bond. The coordinates for missing regions were added with ROSETTA using cyclic coordinate descent[52] and parameters for membrane environments.[53] The resulting models were clustered and the center of these clusters were inspected visually and compared with known structures of class A GPCRs. Depending on structure homology of the known GPCR structures and sequence homology with the target structures, three feasible models were manually selected. In all cases the C- and N-terminal domain was truncated. The final models comprise the TM regions, ICL1, and ECL1 of 2RH1, 1U19, or 2Y00, and the part between the disulfide bridge in ECL2 and TM5 of 3ODU. The remaining parts of the receptors were modeled. The receptor models were refined in full atom representation using the relax protocol.

The receptor-ligand complexes were created with ROSETTA script[54] following the ligand-docking protocol of Davis and Baker[26] with full side chain and backbone flexibility. Ligand placement was allowed within an area of 6 Å radius around the center of the proposed binding site. A total of 4000 models per preceptor subtype were created. The models were sorted by total energy of the complex and clustered with 2 Å RMSD. 950 clusters could be identified for $NPFF_1R$ complexes and 1093 for $NPFF_2R$ complexes. For $NPFF_1R$ the best cluster has -1228 Rosetta Energy Units (REU). The 7th cluster shows the model which agrees with the experimental results. With a energy of -1220 REU it is very close to the best cluster in this docking. For $NPFF_2R$ the best cluster has -1309 REU and the relevant model could be identified in the 12th cluster with -1301 REU. To further verify the ROSETTA results all

complex structures were rescored using the ChemScore function[55] after local optimization. Again, the models were sorted by score and clustered with 2 Å RMSD. 914 clusters could be identified for $NPFF_1R$ complexes and 1134 for $NPFF_2R$ complexes. For $NPFF_1R$ the best cluster has a ChemScore of 34.37. The 8th cluster with a ChemScore of 31.08 shows the model which was selected according to the REU. For $NPFF_2R$ the best cluster has a ChemScore of 34.89. The best model of the 3rd cluster with a ChemScore of 30.03 belongs to the 12th cluster which was selected according to the REU. The scoring by REU and Chemscore is consistent and the presented models are within the top 2% of all produced complex models. The coordinates of the models selected by REU are provided with the supporting information.

SUPPORTING INFORMATION AVAILABLE Experimental details for cytotoxicity profiles of guanidine compounds, cell surface expression of receptor mutants, computational modeling and complex coordinates. This material is available free of charge via the Internet at http://pubs.acs.org.

ACKNOWLEDGMENTS This work was financially supported by a grant from the Deutsche Forschungsgemeinschaft (DFG) (BE1264-11, SFB 610 A1, Z3, IRTG Protein Science) and the Graduate School Leipzig School of Natural Sciences – Building with Molecules and Nano-objects (BuildMoNa). René Meier gratefully thanks for support with computational resources from the ZIH of the TU Dresden. The authors thank K. Löbner for technical support and R. Reppich-Sacher for recording mass spectra. Work in the Meiler lab is supported through grants R01MH090192, R01GM080403 (NIH), and MCB0742762 (NSF).

KEYWORDS. functional selectivity, neuropeptide FF, NPFF receptors, RFamide, small non-peptidic compounds, subtype-selectivity

REFERENCES

1. Yang, H. Y.; Fratta, W.; Majane, E. A.; Costa, E., Isolation, sequencing, synthesis, and pharmacological characterization of two brain neuropeptides that modulate the action of morphine. *Proc. Natl. Acad. Sci. U. S. A.* **1985,** *82*, 7757-7761.

2. Huang, E. Y.; Li, J. Y.; Tan, P. P.; Wong, C. H.; Chen, J. C., The cardiovascular effects of PFRFamide and PFR(Tic)amide, a possible agonist and antagonist of neuropeptide FF (NPFF). *Peptides* **2000,** *21*, 205-210.

3. Laguzzi, R.; Nosjean, A.; Mazarguil, H.; Allard, M., Cardiovascular effects induced by the stimulation of neuropeptide FF receptors in the dorsal vagal complex: an autoradiographic and pharmacological study in the rat. *Brain Res.* **1996,** *711*, 193-202.

4. Fang, Q.; Wang, Y. Q.; He, F.; Guo, J.; Chen, Q.; Wang, R., Inhibition of neuropeptide FF (NPFF)-induced hypothermia and anti-morphine analgesia by RF9, a new selective NPFF receptors antagonist. *Regulatory Peptides* **2008,** *147*, 45-51.

5. Mouledous, L.; Barthas, F.; Zajac, J. M., Opposite control of body temperature by NPFF1 and NPFF2 receptors in mice. *Neuropeptides* **2010,** *44*, 453-456.

6. Kalliomaki, M. L.; Panula, P., Neuropeptide FF, but not prolactin-releasing peptide, mRNA is differentially regulated in the hypothalamic and medullary neurons after salt loading. *Neuroscience* **2004,** *124*, 81-87.

7. Majane, E. A.; Yang, H. Y., Mammalian FMRF-NH2-like peptide in rat pituitary: decrease by osmotic stimulus. *Peptides* **1991,** *12*, 1303-1308.

8. Findeisen, M.; Rathmann, D.; Beck-Sickinger, A. G., RFamide Peptides: Structure, Function, Mechanisms and Pharmaceutical Potential. *Pharmaceuticals* **2011,** *4*, 1248 - 1280.

9. Gouarderes, C.; Tafani, J. A.; Zajac, J. M., Affinity of neuropeptide FF analogs to opioid receptors in the rat spinal cord. *Peptides* **1998,** *19*, 727-730.

10. Raffa, R. B.; Kim, A.; Rice, K. C.; de Costa, B. R.; Codd, E. E.; Rothman, R. B., Low affinity of FMRFamide and four FaRPs (FMRFamide-related peptides), including the mammalian-derived FaRPs F-8-Famide (NPFF) and A-18-Famide, for opioid mu, delta, kappa 1, kappa 2a, or kappa 2b receptors. *Peptides* **1994,** *15*, 401-404.

11. Bonini, J. A.; Jones, K. A.; Adham, N.; Forray, C.; Artymyshyn, R.; Durkin, M. M.; Smith, K. E.; Tamm, J. A.; Boteju, L. W.; Lakhlani, P. P.; Raddatz, R.; Yao, W. J.; Ogozalek, K. L.; Boyle, N.; Kouranova, E. V.; Quan, Y.; Vaysse, P. J.; Wetzel, J. M.; Branchek, T. A.; Gerald, C.; Borowsky, B., Identification and characterization of two G protein-coupled receptors for neuropeptide FF. *J. Biol. Chem.* **2000,** *275*, 39324-39331.

12. Hinuma, S.; Shintani, Y.; Fukusumi, S.; Iijima, N.; Matsumoto, Y.; Hosoya, M.; Fujii, R.; Watanabe, T.; Kikuchi, K.; Terao, Y.; Yano, T.; Yamamoto, T.; Kawamata, Y.; Habata, Y.; Asada, M.; Kitada, C.; Kurokawa, T.; Onda, H.; Nishimura, O.; Tanaka, M.; Ibata, Y.; Fujino, M., New neuropeptides containing carboxy-terminal RFamide and their receptor in mammals. *Nat. Cell Biol.* **2000,** *2*, 703-708.

13. Liu, Q.; Guan, X. M.; Martin, W. J.; McDonald, T. P.; Clements, M. K.; Jiang, Q.; Zeng, Z.; Jacobson, M.; Williams, D. L., Jr.; Yu, H.; Bomford, D.; Figueroa, D.; Mallee, J.; Wang, R.; Evans, J.; Gould, R.; Austin, C. P., Identification and characterization of novel mammalian neuropeptide FF-like peptides that attenuate morphine-induced antinociception. *J. Biol. Chem.* **2001,** *276*, 36961-36969.

14. Perry, S. J.; Yi-Kung Huang, E.; Cronk, D.; Bagust, J.; Sharma, R.; Walker, R. J.; Wilson, S.; Burke, J. F., A human gene encoding morphine modulating peptides related to NPFF and FMRFamide. *FEBS Lett.* **1997,** *409*, 426-430.

15. Vilim, F. S.; Aarnisalo, A. A.; Nieminen, M. L.; Lintunen, M.; Karlstedt, K.; Kontinen, V. K.; Kalso, E.; States, B.; Panula, P.; Ziff, E., Gene for pain modulatory neuropeptide NPFF: induction in spinal cord by noxious stimuli. *Mol. Pharmacol.* **1999,** *55*, 804-811.

16. Gouarderes, C.; Quelven, I.; Mollereau, C.; Mazarguil, H.; Rice, S. Q.; Zajac, J. M., Quantitative autoradiographic distribution of NPFF1 neuropeptide FF receptor in the rat brain and comparison with

NPFF2 receptor by using [125I]YVP and [(125I]EYF as selective radioligands. *Neuroscience* **2002,** *115*, 349-361.

17. Lameh, J.; Bertozzi, F.; Kelly, N.; Jacobi, P. M.; Nguyen, D.; Bajpai, A.; Gaubert, G.; Olsson, R.; Gardell, L. R., Neuropeptide FF receptors have opposing modulatory effects on nociception. *J. Pharmacol. Exp. Ther.* **2010,** *334*, 244-254.

18. Gaubert, G.; Bertozzi, F.; Kelly, N. M.; Pawlas, J.; Scully, A. L.; Nash, N. R.; Gardell, L. R.; Lameh, J.; Olsson, R., Discovery of selective nonpeptidergic neuropeptide FF2 receptor agonists. *J. Med. Chem.* **2009,** *52*, 6511-6514.

19. Fang, Q.; Guo, J.; He, F.; Peng, Y. L.; Chang, M.; Wang, R., In vivo inhibition of neuropeptide FF agonism by BIBP3226, an NPY Y1 receptor antagonist. *Peptides* **2006,** *27*, 2207-2213.

20. Mollereau, C.; Mazarguil, H.; Marcus, D.; Quelven, I.; Kotani, M.; Lannoy, V.; Dumont, Y.; Quirion, R.; Detheux, M.; Parmentier, M.; Zajac, J. M., Pharmacological characterization of human NPFF(1) and NPFF(2) receptors expressed in CHO cells by using NPY Y(1) receptor antagonists. *Eur. J. Pharmacol.* **2002,** *451*, 245-256.

21. Simonin, F.; Schmitt, M.; Laulin, J. P.; Laboureyras, E.; Jhamandas, J. H.; MacTavish, D.; Matifas, A.; Mollereau, C.; Laurent, P.; Parmentier, M.; Kieffer, B. L.; Bourguignon, J. J.; Simonnet, G., RF9, a potent and selective neuropeptide FF receptor antagonist, prevents opioid-induced tolerance associated with hyperalgesia. *Proc. Natl. Acad. Sci. U. S. A.* **2006,** *103*, 466-471.

22. Findeisen, M.; Rathmann, D.; Beck-Sickinger, A. G., Structure-activity studies of RFamide peptides reveal subtype-selective activation of neuropeptide FF1 and FF2 receptors. *ChemMedChem* **2011,** *6*, 1081-1093.

23. Lindner, D.; van Dieck, J.; Merten, N.; Morl, K.; Gunther, R.; Hofmann, H. J.; Beck-Sickinger, A. G., GPC receptors and not ligands decide the binding mode in neuropeptide Y multireceptor/multiligand system. *Biochemistry* **2008,** *47*, 5905-5914.

24. Merten, N.; Lindner, D.; Rabe, N.; Rompler, H.; Morl, K.; Schoneberg, T.; Beck-Sickinger, A. G., Receptor subtype-specific docking of Asp6.59 with C-terminal arginine residues in Y receptor ligands. *J. Biol. Chem.* **2007,** *282*, 7543-7551.

25. Ballesteros, J. A.; Weinstein, H., Integrated methods for the construction of three-dimensional models and computational probing of structure-function relations in G protein-coupled receptors. *Methods Neurosci.* **1995,** *25*, 366-428.

26. Davis, I. W.; Baker, D., RosettaLigand docking with full ligand and receptor flexibility. *J. Mol. Biol.* **2009,** *385*, 381-392.

27. Mollereau, C.; Gouarderes, C.; Dumont, Y.; Kotani, M.; Detheux, M.; Doods, H.; Parmentier, M.; Quirion, R.; Zajac, J. M., Agonist and antagonist activities on human NPFF(2) receptors of the NPY ligands GR231118 and BIBP3226. *Br. J. Pharmacol.* **2001,** *133*, 1-4.

28. Engstrom, M.; Wurster, S.; Savola, J. M.; Panula, P., Functional properties of Pfr(Tic)amide and BIBP3226 at human neuropeptide FF2 receptors. *Peptides* **2003,** *24*, 1947-1954.

29. Rudolf, K.; Eberlein, W.; Engel, W.; Wieland, H. A.; Willim, K. D.; Entzeroth, M.; Wienen, W.; Beck-Sickinger, A. G.; Doods, H. N., The first highly potent and selective non-peptide neuropeptide Y Y1 receptor antagonist: BIBP3226. *Eur. J. Pharmacol.* **1994,** *271*, R11-13.

30. Sautel, M.; Rudolf, K.; Wittneben, H.; Herzog, H.; Martinez, R.; Munoz, M.; Eberlein, W.; Engel, W.; Walker, P.; Beck-Sickinger, A. G., Neuropeptide Y and the nonpeptide antagonist BIBP 3226 share an overlapping binding site at the human Y1 receptor. *Mol. Pharmacol.* **1996,** *50*, 285-292.

31. McAllister, S. D.; Tao, Q.; Barnett-Norris, J.; Buehner, K.; Hurst, D. P.; Guarnieri, F.; Reggio, P. H.; Nowell Harmon, K. W.; Cabral, G. A.; Abood, M. E., A critical role for a tyrosine residue in the cannabinoid receptors for ligand recognition. *Biochem. Pharmacol.* **2002,** *63*, 2121-2136.

32. Berg, K. A.; Maayani, S.; Goldfarb, J.; Scaramellini, C.; Leff, P.; Clarke, W. P., Effector pathway-dependent relative efficacy at serotonin type 2A and 2C receptors: evidence for agonist-directed trafficking of receptor stimulus. *Mol. Pharmacol.* **1998,** *54*, 94-104.

33. McLaughlin, J. N.; Shen, L.; Holinstat, M.; Brooks, J. D.; Dibenedetto, E.; Hamm, H. E., Functional selectivity of G protein signaling by agonist peptides and thrombin for the protease-activated receptor-1. *J. Biol. Chem.* **2005,** *280*, 25048-25059.

34. Urban, J. D.; Clarke, W. P.; von Zastrow, M.; Nichols, D. E.; Kobilka, B.; Weinstein, H.; Javitch, J. A.; Roth, B. L.; Christopoulos, A.; Sexton, P. M.; Miller, K. J.; Spedding, M.; Mailman, R. B., Functional selectivity and classical concepts of quantitative pharmacology. *J. Pharmacol. Exp. Ther.* **2007,** *320*, 1-13.

35. Raehal, K. M.; Schmid, C. L.; Groer, C. E.; Bohn, L. M., Functional selectivity at the mu-opioid receptor: implications for understanding opioid analgesia and tolerance. *Pharmacol. Rev.* **2011,** *63*, 1001-1019.

36. Robb, S.; Cheek, T. R.; Hannan, F. L.; Hall, L. M.; Midgley, J. M.; Evans, P. D., Agonist-specific coupling of a cloned Drosophila octopamine/tyramine receptor to multiple second messenger systems. *EMBO J.* **1994,** *13*, 1325-1330.

37. Rihakova, L.; Quiniou, C.; Hamdan, F. F.; Kaul, R.; Brault, S.; Hou, X.; Lahaie, I.; Sapieha, P.; Hamel, D.; Shao, Z.; Gobeil, F., Jr.; Hardy, P.; Joyal, J. S.; Nedev, H.; Duhamel, F.; Beauregard, K.; Heveker, N.; Saragovi, H. U.; Guillon, G.; Bouvier, M.; Lubell, W. D.; Chemtob, S., VRQ397 (CRAVKY): a novel noncompetitive V2 receptor antagonist. *Am. J. Physiol. Regul. Integr. Comp. Physiol.* **2009,** *297*, R1009-1018.

38. Kilts, J. D.; Connery, H. S.; Arrington, E. G.; Lewis, M. M.; Lawler, C. P.; Oxford, G. S.; O'Malley, K. L.; Todd, R. D.; Blake, B. L.; Nichols, D. E.; Mailman, R. B., Functional selectivity of dopamine receptor agonists. II. Actions of dihydrexidine in D2L receptor-transfected MN9D cells and pituitary lactotrophs. *J. Pharmacol. Exp. Ther.* **2002,** *301*, 1179-1189.

39. Mottola, D. M.; Kilts, J. D.; Lewis, M. M.; Connery, H. S.; Walker, Q. D.; Jones, S. R.; Booth, R. G.; Hyslop, D. K.; Piercey, M.; Wightman, R. M.; Lawler, C. P.; Nichols, D. E.; Mailman, R. B., Functional selectivity of dopamine receptor agonists. I. Selective activation of postsynaptic dopamine D2 receptors linked to adenylate cyclase. *J. Pharmacol. Exp. Ther.* **2002,** *301*, 1166-1178.

40. Ghanouni, P.; Gryczynski, Z.; Steenhuis, J. J.; Lee, T. W.; Farrens, D. L.; Lakowicz, J. R.; Kobilka, B. K., Functionally different agonists induce distinct conformations in the G protein coupling domain of the beta 2 adrenergic receptor. *J. Biol. Chem.* **2001,** *276*, 24433-24436.

41. Ebersole, B. J.; Visiers, I.; Weinstein, H.; Sealfon, S. C., Molecular basis of partial agonism: orientation of indoleamine ligands in the binding pocket of the human serotonin 5-HT2A receptor determines relative efficacy. *Mol. Pharmacol.* **2003,** *63*, 36-43.

42. Kurrasch-Orbaugh, D. M.; Watts, V. J.; Barker, E. L.; Nichols, D. E., Serotonin 5-hydroxytryptamine 2A receptor-coupled phospholipase C and phospholipase A2 signaling pathways have different receptor reserves. *J. Pharmacol. Exp. Ther.* **2003,** *304*, 229-237.

43. Gouarderes, C.; Mazarguil, H.; Mollereau, C.; Chartrel, N.; Leprince, J.; Vaudry, H.; Zajac, J. M., Functional differences between NPFF1 and NPFF2 receptor coupling: high intrinsic activities of RFamide-related peptides on stimulation of [35S]GTPgammaS binding. *Neuropharmacology* **2007,** *52*, 376-386.

44. Lebon, G.; Warne, T.; Edwards, P. C.; Bennett, K.; Langmead, C. J.; Leslie, A. G.; Tate, C. G., Agonist-bound adenosine A2A receptor structures reveal common features of GPCR activation. *Nature* **2011,** *474*, 521-525.

45. Wu, B.; Chien, E. Y.; Mol, C. D.; Fenalti, G.; Liu, W.; Katritch, V.; Abagyan, R.; Brooun, A.; Wells, P.; Bi, F. C.; Hamel, D. J.; Kuhn, P.; Handel, T. M.; Cherezov, V.; Stevens, R. C., Structures of the CXCR4 chemokine GPCR with small-molecule and cyclic peptide antagonists. *Science* **2010,** *330*, 1066-1071.

46. Cherezov, V.; Rosenbaum, D. M.; Hanson, M. A.; Rasmussen, S. G.; Thian, F. S.; Kobilka, T. S.; Choi, H. J.; Kuhn, P.; Weis, W. I.; Kobilka, B. K.; Stevens, R. C., High-resolution crystal structure of an engineered human beta2-adrenergic G protein-coupled receptor. *Science* **2007,** *318*, 1258-1265.

47. Okada, T.; Sugihara, M.; Bondar, A. N.; Elstner, M.; Entel, P.; Buss, V., The retinal conformation and its environment in rhodopsin in light of a new 2.2 A crystal structure. *J. Mol. Biol.* **2004,** *342*, 571-583.

48. Warne, T.; Moukhametzianov, R.; Baker, J. G.; Nehme, R.; Edwards, P. C.; Leslie, A. G.; Schertler, G. F.; Tate, C. G., The structural basis for agonist and partial agonist action on a beta(1)-adrenergic receptor. *Nature* **2011,** *469*, 241-244.

49. Shimamura, T.; Shiroishi, M.; Weyand, S.; Tsujimoto, H.; Winter, G.; Katritch, V.; Abagyan, R.; Cherezov, V.; Liu, W.; Han, G. W.; Kobayashi, T.; Stevens, R. C.; Iwata, S., Structure of the human histamine H1 receptor complex with doxepin. *Nature* **2011,** *475*, 65-70.

50. Murakami, M.; Kouyama, T., Crystal structure of squid rhodopsin. *Nature* **2008,** *453*, 363-367.

51. Chien, E. Y.; Liu, W.; Zhao, Q.; Katritch, V.; Han, G. W.; Hanson, M. A.; Shi, L.; Newman, A. H.; Javitch, J. A.; Cherezov, V.; Stevens, R. C., Structure of the human dopamine D3 receptor in complex with a D2/D3 selective antagonist. *Science* **2010,** *330*, 1091-1095.

52. Canutescu, A. A.; Dunbrack, R. L., Jr., Cyclic coordinate descent: A robotics algorithm for protein loop closure. *Protein Sci.* **2003,** *12*, 963-972.

53. Barth, P.; Schonbrun, J.; Baker, D., Toward high-resolution prediction and design of transmembrane helical protein structures. *Proc. Natl. Acad. Sci. U. S. A.* **2007,** *104*, 15682-15687.

54. Fleishman, S. J.; Leaver-Fay, A.; Corn, J. E.; Strauch, E. M.; Khare, S. D.; Koga, N.; Ashworth, J.; Murphy, P.; Richter, F.; Lemmon, G.; Meiler, J.; Baker, D., RosettaScripts: a scripting language interface to the Rosetta macromolecular modeling suite. *PLoS One* **2011,** *6*, e20161.

55. Baxter, C. A.; Murray, C. W.; Clark, D. E.; Westhead, D. R.; Eldridge, M. D., Flexible docking using Tabu search and an empirical estimate of binding affinity. *Proteins* **1998,** *33*, 367-382.

SYNOPSIS TOC

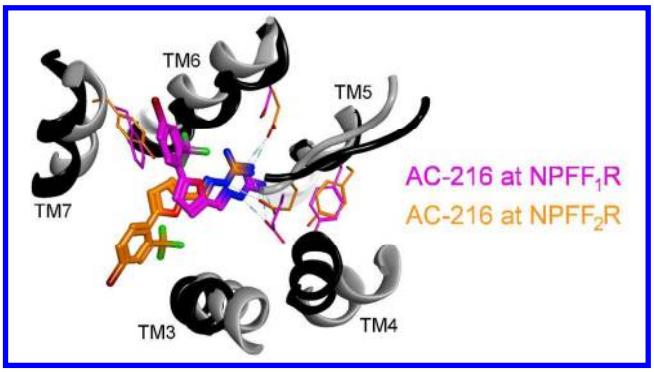

Supporting Information

Selective mode of action of guanidine-containing non-peptides at human NPFF receptors

Maria Findeisen[†,⊥], *Cäcilia Würker*[†,⊥], *Daniel Rathmann*[†], *René Meier*[†], *Jens Meiler*[‡], *Roger Olsson*[§] *and Annette G. Beck-Sickinger**[†]

† Institute of Biochemistry, Faculty of Biosciences, Pharmacy and Psychology, Leipzig University, Brüderstrasse 34, D-04103 Leipzig, Germany

‡ Vanderbilt University, Center for Structural Biology, 5144B Biosci/MRBIII, 465 21st Avenue South, Nashville, TN 37232-8725, USA

§ ACADIA Pharmaceuticals Inc., 3911 Sorrento Valley Boulevard, San Diego, California 92121, and Medicinal Chemistry, Faculty of Science, University of Gothenburg, PO Box 460, SE-405 30 Gothenburg, Sweden

Author Contributions.

⊥ These authors contributed equally to this work, joint first authors.

AUTHOR INFORMATION.

To whom correspondence should be addressed. Annette G. Beck-Sickinger, Universität Leipzig, Faculty of Biosciences, Pharmacy and Psychology, Institute of Biochemistry, Brüderstraße 34, 04103 Leipzig, Germany. Phone: 0049-341-9736900. Fax: 0049-341-9736909. E-mail: beck-sickinger@uni-leipzig.de.

Table S1. Results of Resazurin-based Cell Viability Assays for Cytotoxicity Testing.

Compound	IC_{50} (µM)[a]
AC-970	81 ± 2.5
AC-216	60 ± 3.8
AC-093	26 ± 2.3
AC-099	26 ± 3.3

[a]COS-7 cells were stimulated for a defined time period of 2 h with various concentrations of compounds and controls (FCS, Ethanol). After stimulation IC_{50} values were obtained using nonlinear regression. Values are the mean (± SEM) of parameters deduced by using Prism 3.0 software.

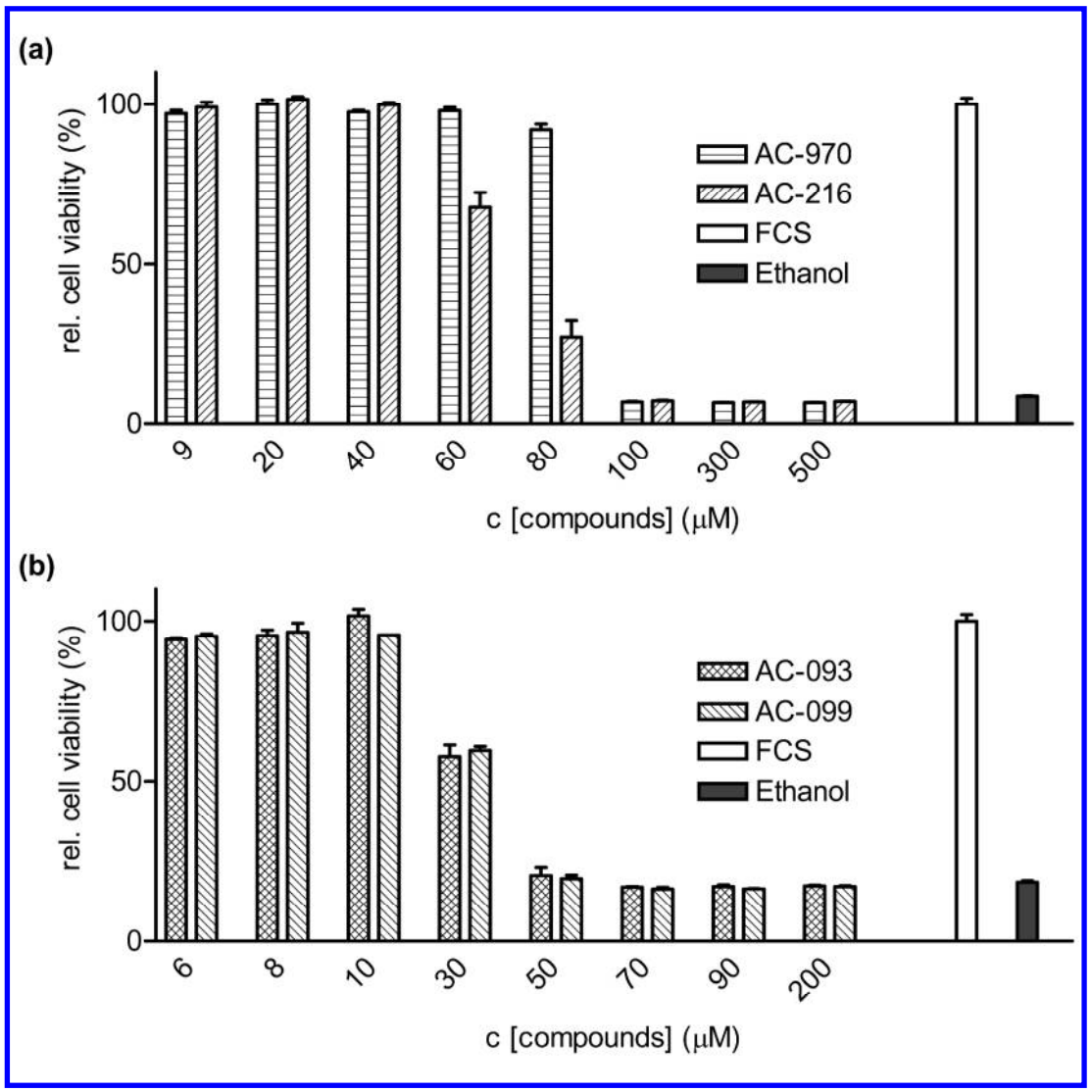

Figure S1. The reported cytotoxicity profiles were obtained by performing Resazurin-based cell viability assays using COS-7 cells. Results shown indicate a cytotoxic effect of small compounds AC-970 and AC-216 (panel a) as well as AC-093 and AC-099 (panel b) due to decreasing relative cell viability at high compound concentrations. The cytotoxicity profiles were obtained from data of two independent experiments performed in triplicates and were used to generate IC_{50} values which are summarized in Table S1.

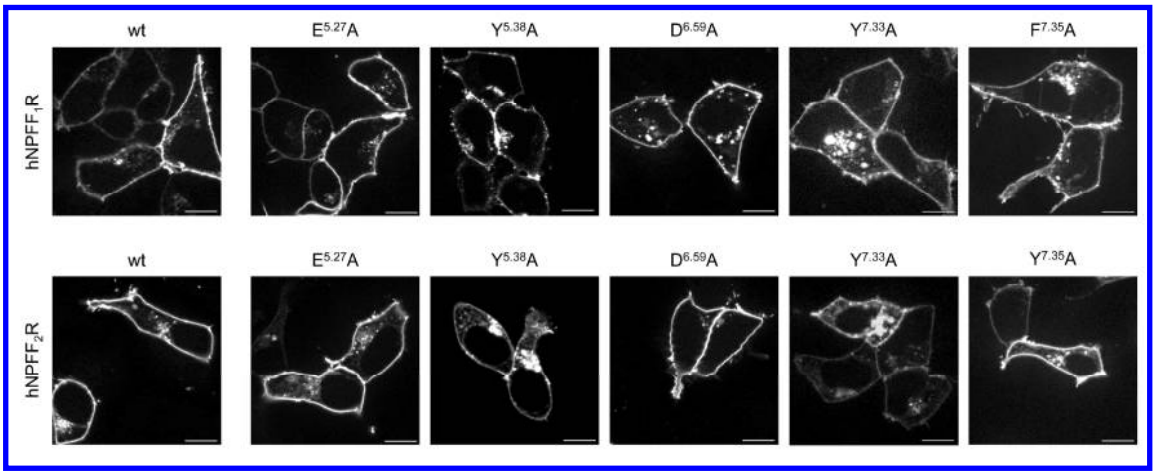

Figure S2. Cell surface expression of Ala mutants of $NPFF_{1/2}R$. HEK293 cells were transiently transfected with different NPFFR mutants C-terminally fused to EYFP. Scale bars represent 10 µm.

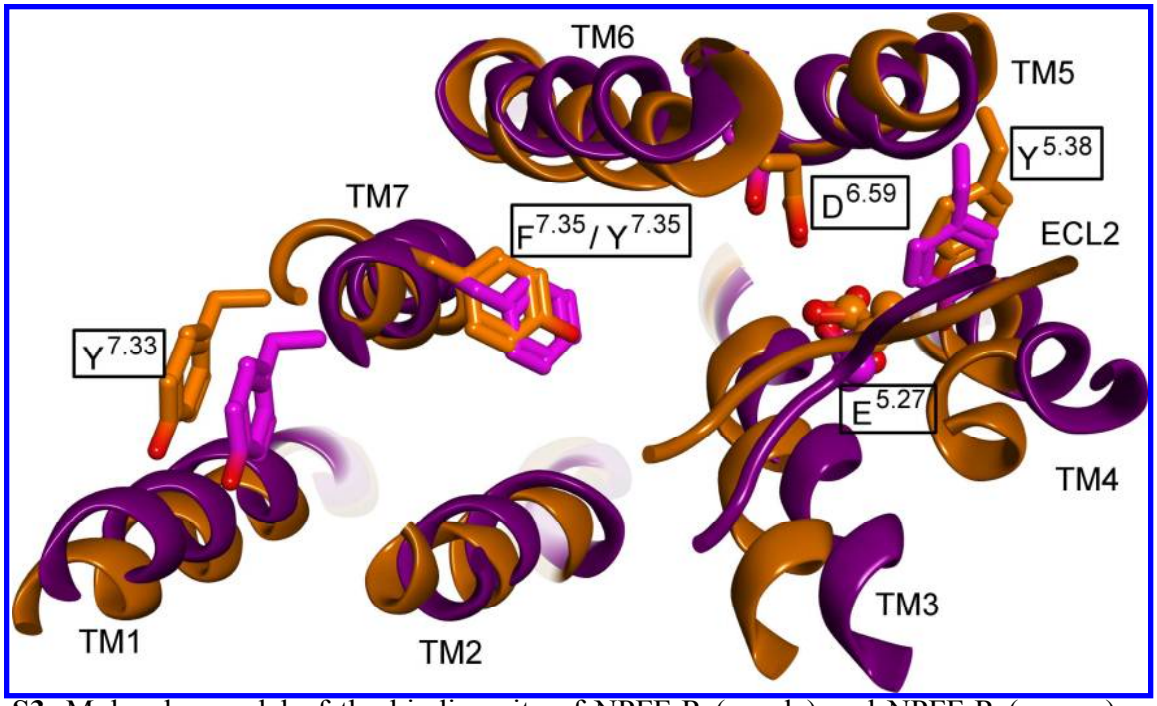

Figure S3. Molecular model of the binding site of $NPFF_1R$ (purple) and $NPFF_2R$ (orange) as shown from the extracellular side. Depicted are parts of the backbone of the seven TM helices in ribbon representation and the side chains of the amino acids forming the binding pocket in sticks. The amino acids which were known to be important in advance to the model creation are shown in ball and stick representation.

SYNOPSIS TOC

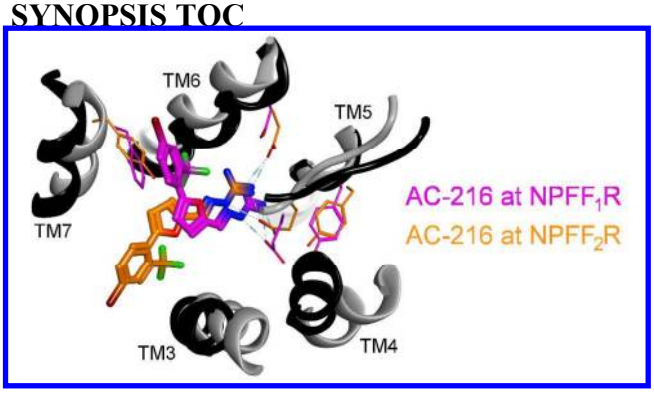

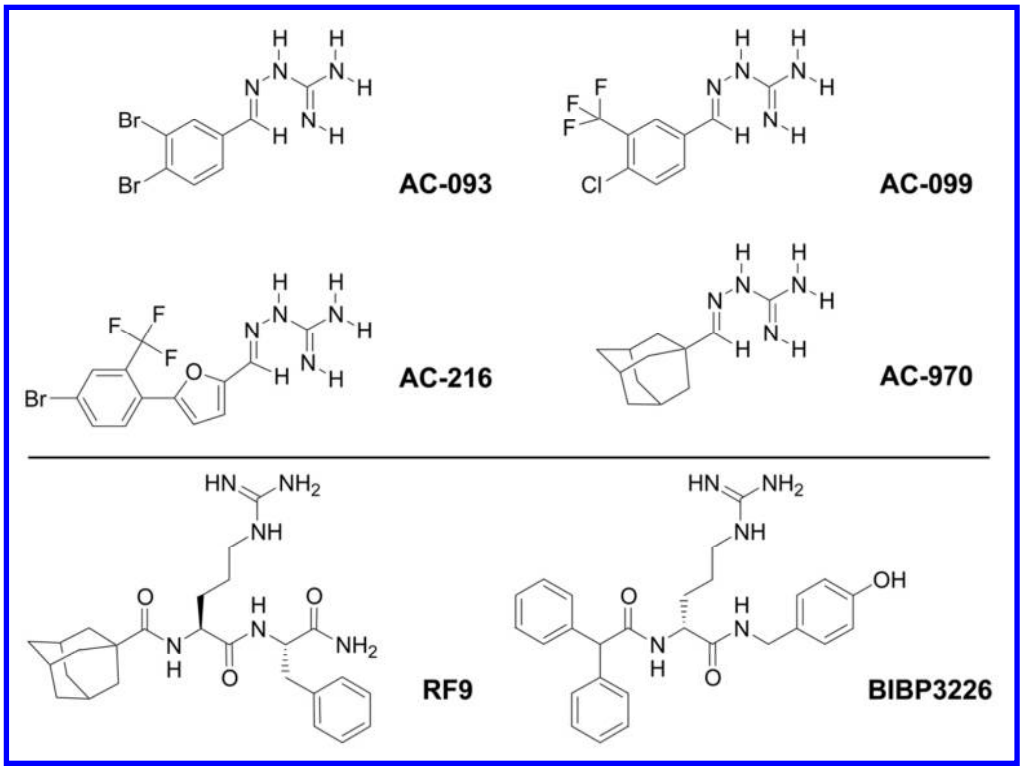

Figure 1. Structures of AC 093, AC 099, AC 216, AC 970, RF9 and BIBP3226.
111x83mm (300 x 300 DPI)

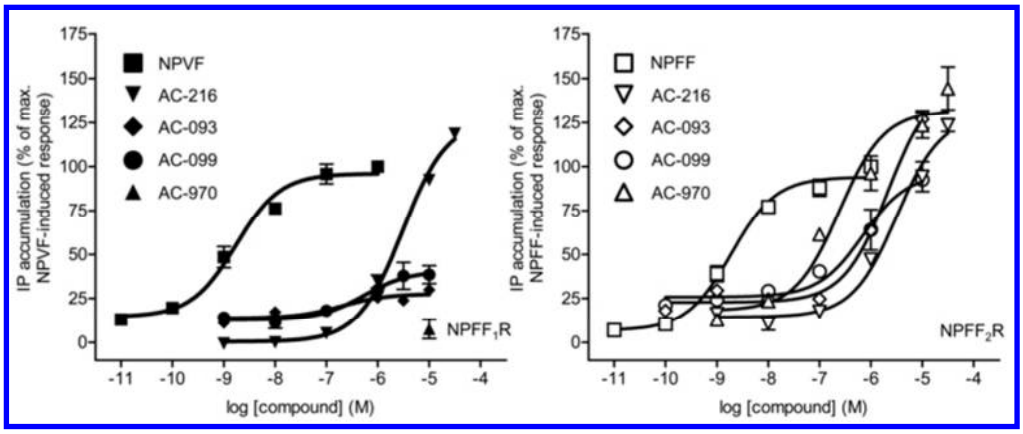

Figure 2. Representative concentration response curves after 2 h of stimulation with small non peptidic ligands AC 093, AC 099, AC 216 and AC 970 and endogenous ligands at human NPFF1R (left panel) and NPFF2R (right panel) in IP signal transduction assays. Results are expressed as percentage relative to maximal IP accumulation of the reference agonists and were obtained in COS 7 cells expressing NPFFR wt and chimeric G-protein as described in the Experimental Section. Concentration-response curves are obtained from data of at least two independent experiments performed in duplicates and were used to generate EC50 and Emax values, which are summarized in Table 1.
61x25mm (300 x 300 DPI)

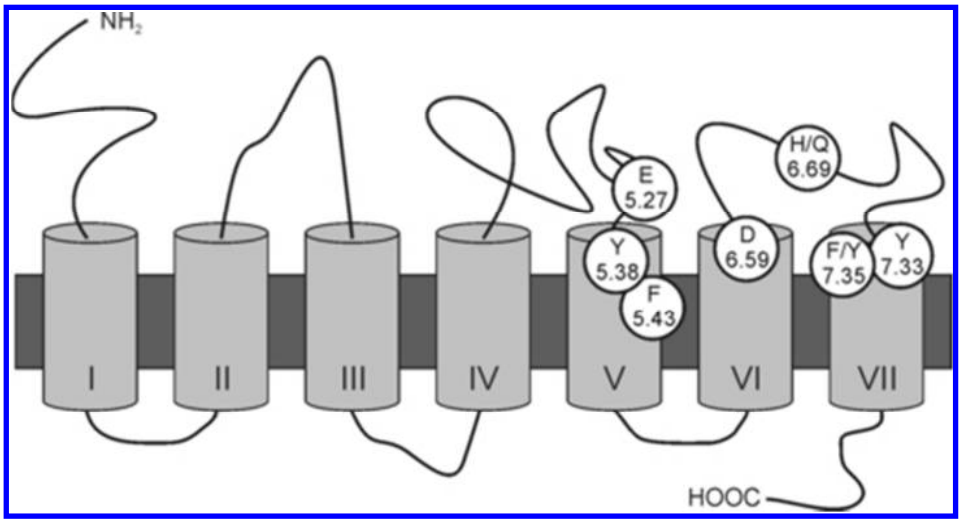

Figure 3. Schematic representation of NPFF receptor topology. Investigated positions are highlighted and numbered according to Ballesteros and Weinstein.
39x21mm (300 x 300 DPI)

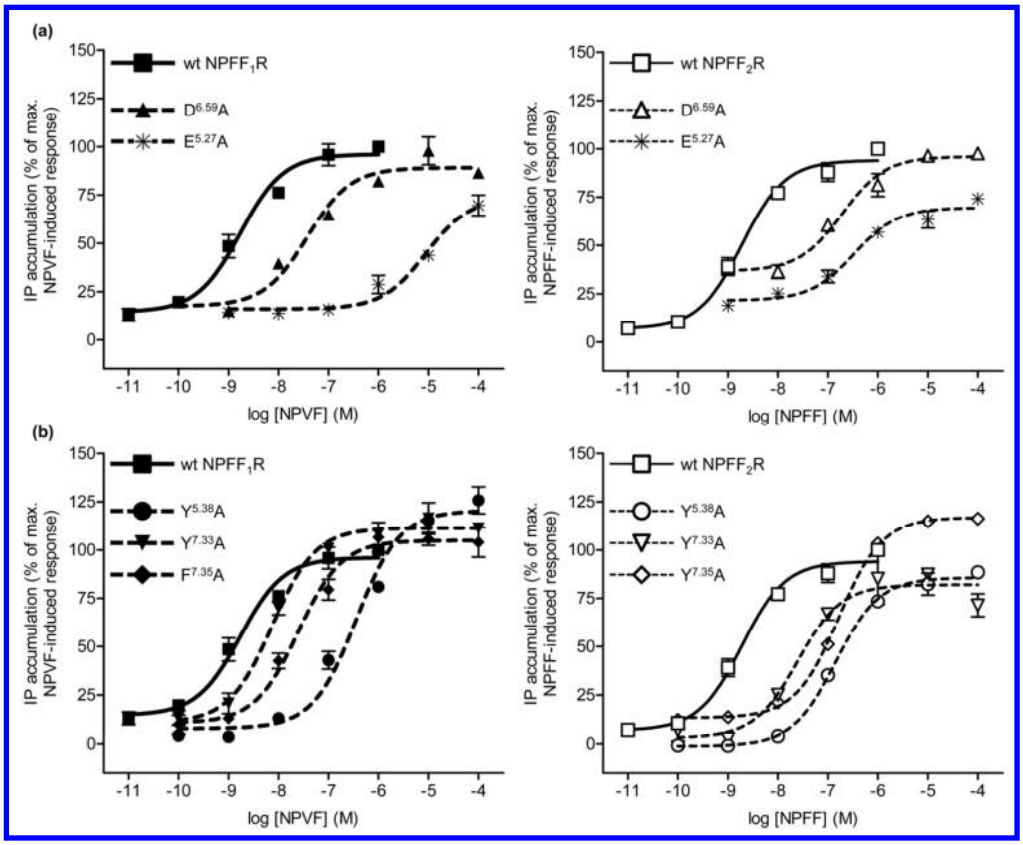

Figure 4. IP signal transduction assays were performed at wt and corresponding receptor mutants of the human NPFF1R (left panels) and NPFF2R (right panels) after stimulation with the endogenous ligands as described in the Experimental Section. Representative concentration response curves are presented for replacement of the negatively charged residues D6.59 and E5.27 (panel a) as well as mutation of the aromatic amino acids Y5.38, Y7.33 and F7.35/Y7.35 (panel b). Results shown are expressed as percentage relative to maximal IP production of the reference agonists and were obtained in COS 7 cells expressing NPFFR wt or mutant construct and chimeric G-protein. Concentration response curves are obtained from data of at least two independent experiments performed in duplicates and were used to generate EC50 and Emax values, which are summarized in Table 2.
123x101mm (300 x 300 DPI)

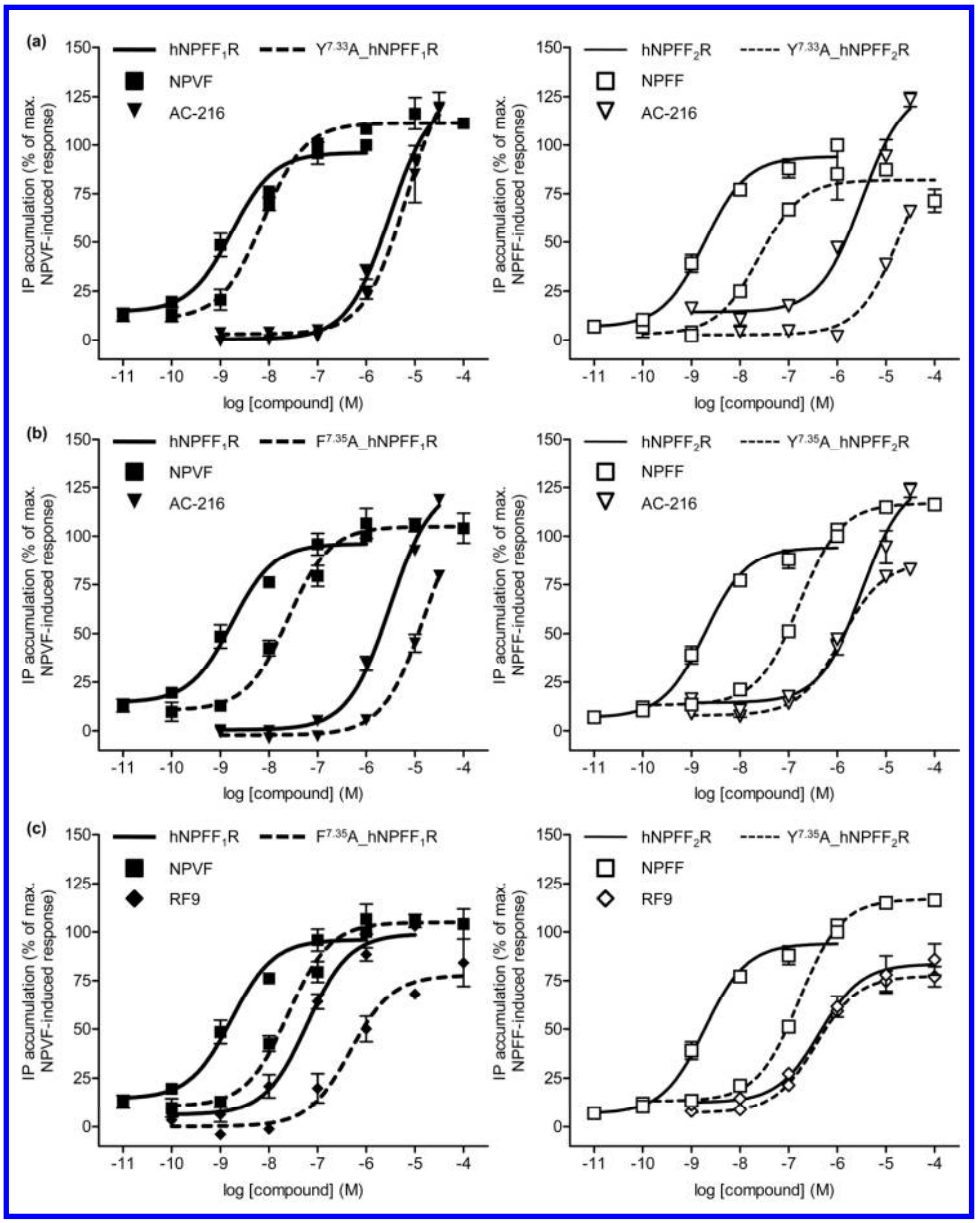

Figure 5. IP signal transduction assays were performed at wt and corresponding receptor mutants of the human NPFF1R (left panels) and NPFF2R (right panels) as described in the Experimental Section. Representative concentration response curves are presented for stimulation of AC 216 at position Y7.33A (panel a) and AC 216 (panel b) and RF9 (panel c) at F7.35A_hNPFF1R and Y7.35A_hNPFF2R, respectively. Obtained data indicate a subtype selective binding mode of AC 216 and RF9 at F7.35A_hNPFF1R and Y7.35A_hNPFF2R, respectively. Results shown are expressed as percentage relative to maximal IP production of the reference agonists and were obtained in COS 7 cells expressing NPFFR wt or mutant construct and chimeric G-protein. Concentration response curves are obtained from data of at least two independent experiments performed in duplicates and were used to generate EC50 and Emax values, which are summarized in Table 2.
187x235mm (300 x 300 DPI)

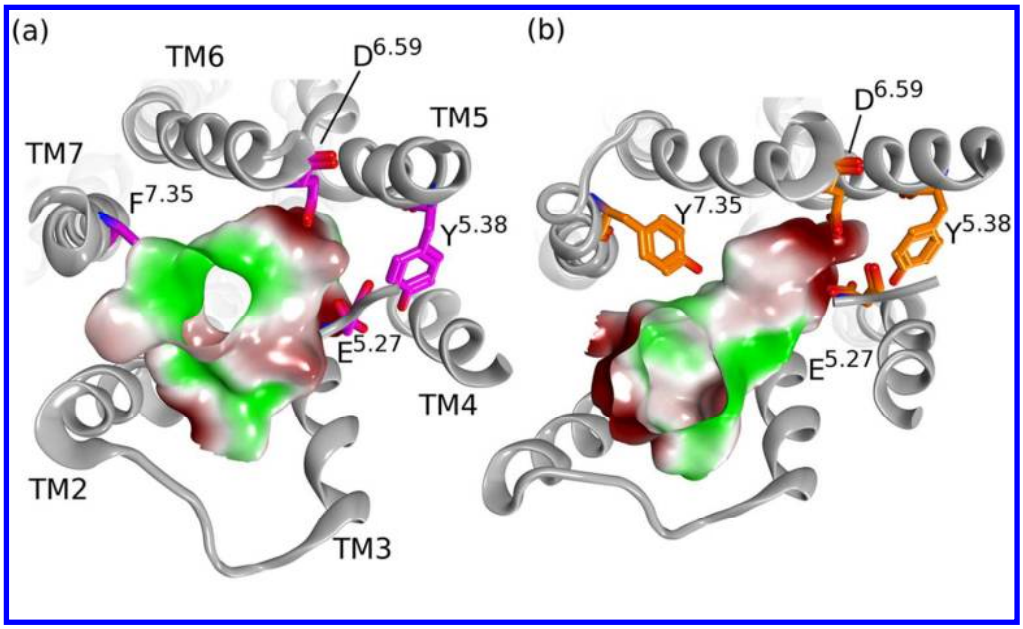

Figure 6. Shape of the binding site in the models of NPFF1R (a) and NPFF2R (b) as shown from the extracellular side. Depicted is the backbone of the receptor models in gray ribbon representation and the important amino acids which form the binding pocket in purple and orange, respectively. The solvent accessible surface of the binding site was calculated with a 1.4 Å water probe and was colored by hydrophobicity. Hydrophobic areas are colored green and hydrophilic areas are colored red.
91x55mm (300 x 300 DPI)

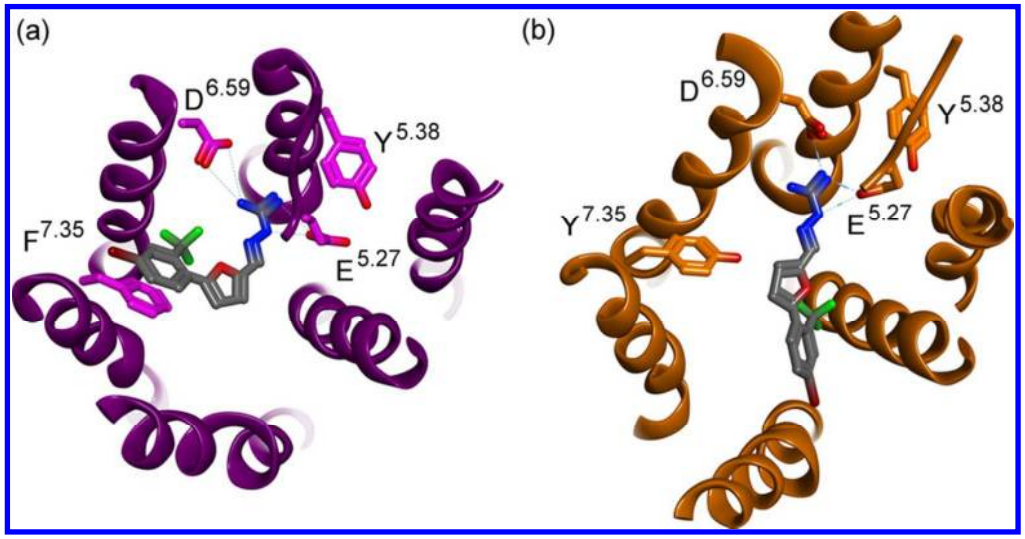

Figure 7. Model of the binding site of NPFF1R and NPFF2R in complex with AC-216. NPFF1R (a) is shown in purple and NPFF2R (b) in orange. Depicted are parts of the backbone of the seven TM helices in ribbon representation and the side chains of the amino acids forming the binding pocket in sticks. The bound ligand AC-216 as predicted from docking is shown in gray sticks.
77x39mm (300 x 300 DPI)

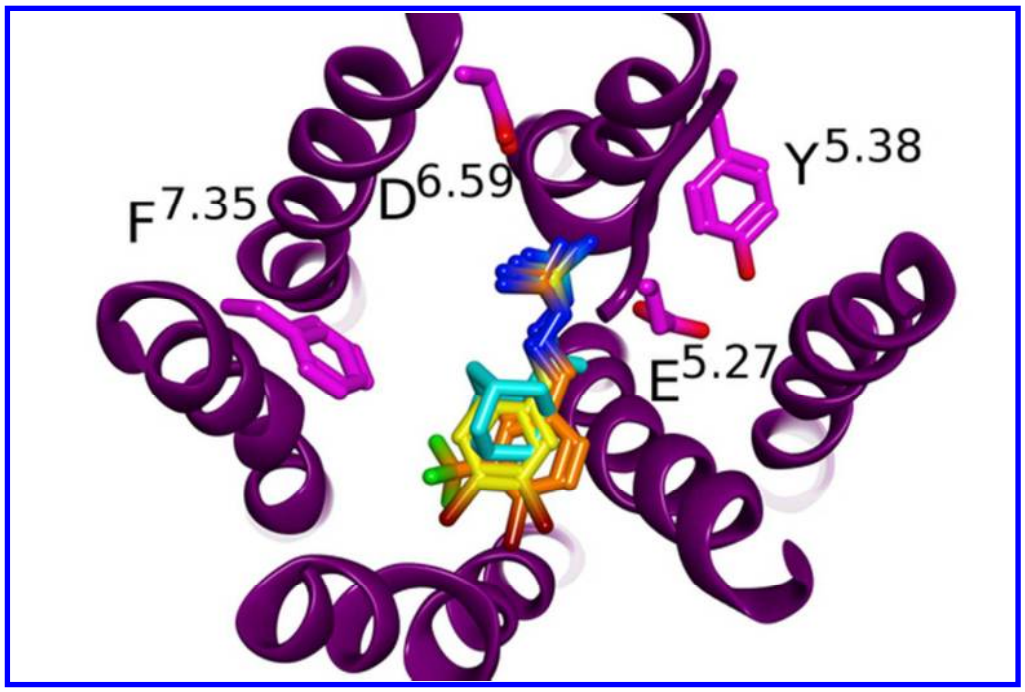

Figure 8. Model of the binding site of NPFF1R in complex with AC-093, AC-099 and AC-970. NPFF1R is shown in purple ribbon representation with its important amino acids highlighted as purple sticks. AC-093 is depicted in yellow sticks, AC-099 in orange sticks and AC-970 in cyan sticks.
49x33mm (300 x 300 DPI)

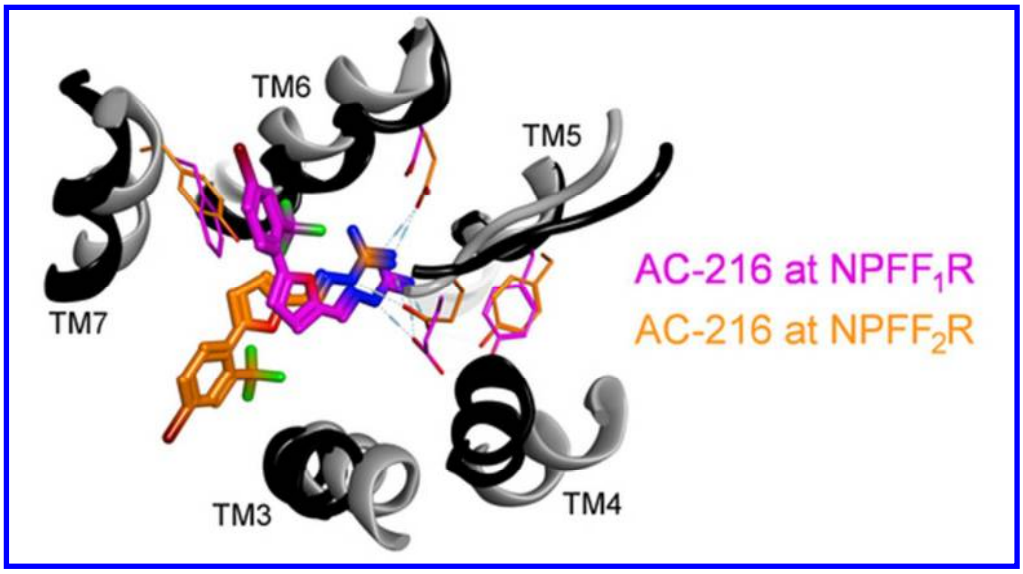

45x25mm (300 x 300 DPI)